



# The Evolution over Time and North–South Asymmetry of Sunspots and Solar Plages for the Period 1910 to 1937 Using Data from Ebro Catalogues

V. de Paula<sup>1</sup> · J.J. Curto<sup>1</sup>

Received: 11 February 2020 / Accepted: 7 June 2020 / Published online: 23 July 2020  
© Springer Nature B.V. 2020

**Abstract** In this work, we analysed both the evolution over time and the north–south (N-S) asymmetry of certain solar features with regards to their morphological type and area. We examined and compared simultaneously 4212 photospheric sunspot groups and 5781 chromospheric solar plage groups using data from the Ebro Observatory catalogues for the period 1910–1937. We found that the most frequently recorded groups of sunspots and solar plages are the smallest ones, and the total number of occurrences of these groups is, on average, about 23% higher for solar plages than for sunspots. Concerning the N-S asymmetry, when the northern hemisphere becomes predominant, it dominates the other hemisphere for a longer time than the opposite case and shows a higher asymmetry. In addition, we found that the normalized N-S asymmetry index,  $\delta$ , of solar activity in terms of the occurrence of sunspots and solar plage groups follows approximately the same behaviour regardless of the morphological type, but presents a slight dependence on their area, since sunspot and solar plage groups show higher values of the  $\delta$  index, the larger their areas are. Furthermore, we noticed three highly significant extremes in the N-S asymmetry, located around the minima of the 14th, 15th and 16th solar cycles (1912 [S]; 1924 [N]; 1933 [N]). However, the general trend is not equal in both structures, since in contrast to sunspots, solar plage groups present lower values of asymmetry throughout practically all the period under consideration. These facts could be interpreted in terms of magnetic cancellation processes and/or merging of close-by faculae.

**Keywords** Sunspots · Cortie classification · Zürich classification · Solar plages · N-S asymmetry

---

✉ J.J. Curto

<sup>1</sup> Observatori de l'Ebre (OE), CSIC-URL, Horta Alta 38, 43520 Roquetes, Spain

## 1. Introduction

The Ebro Observatory has converted their oldest heliophysics catalogues published annually in the period 1910–1937 into a digital format in order to make these data available for computational processing. These catalogues include daily measurements of several parameters of sunspots and solar plages, two different structures located at different layers of the solar atmosphere.

Sunspots are colder dark regions located in the solar photosphere. They originate in intense magnetic fields which form in the solar interior and emanate toward the surface (Weiss, 2001; Kılıçık and Sahin, 2017). Although they might remain visible for several weeks, sunspots usually have lifetimes of less than seven days, and within this time they evolve, changing their position in the solar disc, as well as their size and shape (Solanki, 2003).

Solar plages or flocculi are enormous bright hot regions located in the solar chromosphere that can be observed by isolating one of the wavelengths in which they stand out; that is, the hydrogen H $\alpha$  line (656.3 nm) and the calcium II K line (393.4 nm). These structures are the product of complex magnetic processes and constitute the extension of the photospheric faculae up to the chromosphere. Solar plages tend to originate above regions where a sunspot group will form some time after, and, just like sunspots, they can also change in size and shape within their lifetime, persisting even after the death of their associated sunspot group (Lemaire, 2001; Buehler et al., 2015). The question of historical full-disc observations of solar plages has seen an increasing number of studies over the last few years. This is because they can provide exclusive information about solar magnetic regions and the solar chromosphere. Moreover, they also constitute unique datasets for studying solar activity and solar irradiance, which can improve our knowledge about solar changes in the long-term and solar influence on the Earth's climate (Ermolli et al., 2009, 2018; Chatzistergos et al., 2019a, 2019b).

Solar activity is not equal in both hemispheres. There are significant differences that lead to the so-called north–south (N-S) asymmetry, with the active or preferred hemisphere being the one with the greater solar activity (Hathaway, 2015). The N-S asymmetry was detected for the first time by Spörer (1889) and Maunder (1900; 1904) after noting that sunspot distribution was concentrated in a certain solar hemisphere for long periods of time. From then on, this anomaly has been studied through several solar activity indicators such as the International Sunspot Number and sunspot areas (Newton and Milsom, 1955; Bell, 1962; Waldmeier, 1971; Roy, 1977; Vizoso and Ballester, 1990; Carbonell, Oliver, and Ballester, 1993; Oliver and Ballester, 1994; Temmer et al., 2006; Mandal et al., 2017), solar plage areas (Gonçalves et al., 2014; Mandal, Chatterjee, and Bajernee, 2017), prominences and filaments (Vizoso and Ballester, 1987; Joshi, 1995; Verma, 2000; Gigolashvili et al., 2005), solar flares (García, 1990; Verma, 1992; Temmer et al., 2001; Joshi, Pant, and Manoharan, 2006), and the photospheric and heliospheric magnetic fields (Howard, 1974; Mursula and Hiltula, 2003; Song, Wang, and Ma, 2005; Wang and Robbrecht, 2011). All in all, this suggests that it is worth taking the two hemispheres separately when studying solar activity.

The aim of this paper is to analyse simultaneously the whole set of our sunspot and solar plage data, focusing on their evolution over time and the N-S asymmetry of the daily rate of their occurrence as well as their annual distribution, in relation to the total number of occurrences of each structure type within the different classification schemes, and also regarding the total number of occurrences of each structure within four different area bins. In the case of sunspots, and in order to make a comparison with data sets from other observatories, we have also converted the morphological types of our records from the Cortie classification into the Zürich classification.

## 2. Data

### 2.1. The Ebro Observatory Heliophysics Catalogue

Since its foundation in 1904, the Ebro Observatory has had a solar section specialized in studying Sun–Earth relations. At that time, the observatory had a Mailhat telescope with an equatorial mounting, adapted to take photographs of the Sun for the study of sunspots and prominences (Curto et al., 2016). In order to study the solar calcium plages, the Ebro Observatory also owned an Evershed spectroheliograph (the first in Spain) as well as a Roland spectrogoniometer with a photographic camera (Udías, 2003).

In 1910, the Ebro Observatory began to publish an annual bulletin of its heliophysics catalogue reporting the daily measurements of sunspots and solar plages (focculi). For every daily observation, the sunspot and solar plage parameters recorded were: the group number (N) given in order of appearance; the heliographic latitude ( $\varphi$ ); the heliographic longitudes with respect to the central meridian ( $\lambda$ ), and the first meridian (L); the distance from the centre of the solar disc in hundredths of the radius of the photoheliographic image ( $\rho$ ); the area in mm<sup>2</sup> referred to a 200 mm-diameter plate (S.M.); the reduced or real area (S.R.), in millionths of a solar hemisphere (MSH) for sunspots, and in hundred thousandths of a solar hemisphere (100 KSH) for solar plages; and the morphological class or type of each observed occurrence, in the Cortie classification scheme for sunspots, and in a particular classification for solar plages developed by the Ebro Observatory (“Clase”, meaning class or type). As in our sources “class” and “type” terms were used indistinctly, from now on we will do the same. For detailed information, a copy of the original bulletins can be found in: <http://www.obsebre.es/en/observatori-publicacions>.

The series of records for both sunspots and solar plages were interrupted at the end of 1937 because of the Spanish Civil War (1936–1939), and only the sunspot equipment was maintained and kept in use after the conflict (Romañá, 1942). The observatory continued to collect sunspot daily records from 1942 up to 2000, when the Mailhat instrument was replaced by a Zeiss APQ telescope, which is still operational nowadays (Curto et al., 2016). Despite several attempts to fix the solar plage equipment (Romañá, 1947), solar plage records came to an end in 1937. However, thanks to the tracking of 5781 groups and 33 357 rows of data entries, it still represents one of the longest solar plage series ever collected. In the case of sunspots, the series for the same period up to 1937 has 20 954 rows of data entries belonging to 4212 sunspot groups.

All the heliophysics catalogues from 1910 to 1937 (both inclusive) have been scanned as images and introduced into an optical character recognition program (OCR) in order to convert the data into the ASCII format. In the conversion process, some characters were not correctly converted, so a manual inspection of the data was also done (Curto et al., 2016).

In this work, we have focused on the records of the morphological type, heliographic position, and area of the sunspots and solar plage groups registered between 1910 and 1937, which correspond to the end of the 14th solar cycle, the entire 15th and 16th solar cycles, and the beginning and maximum of the 17th solar cycle.

### 2.2. Sunspot Classification

In the mid-18th century, most astronomical observatories began to publish their first sunspot catalogues with daily records and detailed information (Stephenson, 1990; Lefèvre and Clette, 2014). These catalogues, however, used their own classification schemes and criteria

**Table 1** Cortie classification of sunspot groups (Cortie, 1901).

Type I	Group of one or more small scattered spots.
Type IIa	Group with a two-spot formation in which the leading spot is the principal one.
Type IIb	Group with a two-spot formation in which the trailing spot is the principal one.
Type IIc	Group with a two-spot formation in which both spots are principal.
Type IIIa	Train of spots with well-defined principal spots.
Type IIIb	Train of penumbral spots with irregular umbra and without well-defined principal spots.
Type IVa	Single spot with round and regular outline.
Type IVb	Single spot with regular outline and small companions.
Type IVc	Single spot with irregular outline.
Type IVd	Single spot with irregular outline and train of small companions.
Type IVe	Single spot with irregular outline and small companions but not in a train.
Type V	Irregular group of large spots.

**Table 2** Zürich classification of sunspot groups (Waldmeier, 1947).

Type A	One or more spots without penumbra, and without bipolar configuration.
Type B	Group of spots without penumbra, with bipolar configuration.
Type C	Bipolar group which contains one spot with penumbra.
Type D	Bipolar group whose main spot have penumbra; length less than $10^\circ$ .
Type E	Bipolar group whose main spot have penumbra; length between $10^\circ$ and $15^\circ$ .
Type F	Large bipolar group; length greater than $15^\circ$ .
Type G	Bipolar group with penumbras and no small spots between the main spot; length greater than $10^\circ$ .
Type H	Single spot with penumbra and diameter larger than $2.5^\circ$ .
Type J	Single spot with penumbra and diameter smaller than $2.5^\circ$ .

so, in order to promote sunspot investigation and unify the different classifications, Aloysius Cortie (1901) proposed a scheme of five main types with several subtypes of sunspot groups, organized according to their morphology and evolutionary state (Table 1). This is the so-called Cortie classification. As reported by Cortie, the common evolutionary sequence of a sunspot group was: *I-IIb-IIa-IIIa-IIa-IVd-IVa-I* (Cortie, 1901).

The Ebro Observatory also adopted this classification in their sunspot catalogues when they first began publishing them. However, some subtypes present a very small number of observed occurrences per year. Since a low number of occurrences are not statistically significant, in Section 3 we have grouped those types in the Cortie classification with similar characteristics. Hence, the original 12 types and subtypes have been reduced to five classes: the subtypes from Type *II* have been grouped together, and the same procedure has been followed for Types *III* and *IV*. Type *I* and *V* do not have any common characteristic with the others and, thus, have been maintained.

Over time, the Cortie classification was substituted by the Zürich classification, developed by Max Waldmeier (1947). This 9-type scheme also organized the sunspot groups according to their shape and evolutionary state (Table 2). In this classification, the habitual sequence of a sunspot group would begin with the *A* Type, and then it might or might not evolve through the *B*, *C*, *D*, *E*, *F*, *G*, *H* and *J* Types (Waldmeier, 1947).

One of the most important differences between the Cortie and Zürich classifications is that the latter allowed us to relate the appearance of certain types of sunspot groups to solar flares. Specifically, the Zürich classification predicted a higher probability of the occurrence

**Table 3** Percentages of the Cortie types at the Ebro Observatory (this study) and Kodaikanal Observatory (Ananthakrishnan, 1952) for the coincident period (1910–1937), and the Valencia Observatory (Carrasco et al., 2015) for the period 1920–1928.

Cortie type	Ebro (1910–1937)	Kodaikanal (1910–1937)	Valencia (1920–1928)
I	41.4%	62.9%	45.0%
II	7.1%	2.2%	5.8%
III	15.8%	8.2%	4.4%
IV	32.1%	25.2%	34.2%
V	3.6%	1.4%	10.6%

of flares with Types *D*, *E* and *F*. However, the correlation with these phenomena was quite low, which led to the revision of the method and the introduction of the McIntosh classification (1990). This classification is the one currently in use and is composed of three parameters or components (*Zpc*), whose combination allows us to obtain 60 different types of sunspot groups. Thus, *Z* component organizes the sunspot groups according to seven different configuration types and consists in a revision of the Zürich classification mainly types; *p* characterizes the penumbra of the largest sunspot of the group into six types; finally, *c* parameter references to four types of possible distributions of the sunspots within the groups.

In order to interpret and obtain additional information in sunspot records prior to the Zürich classification, Carrasco et al. (2015) proposed an equivalence between the Cortie and Zürich classifications. They suggested a set of conditions that the sunspot groups in the Cortie classification needed to meet to be assigned to a particular Zürich type and they implemented these conditions to an 8-year series of records from the sunspot catalogue of the Valencia University Observatory (from 1920 to 1928).

Likewise, we converted the Ebro Observatory sunspot records from the period 1910–1937, originally in the Cortie type, into the Zürich class by using the same criteria that Carrasco et al. (2015) employed in their article. Then, we compared our data with other series belonging to different observatories. Figure 1 shows the percentage of each type for both classifications of the records in the Ebro Observatory catalogue. As with the Valencia Observatory data, the greatest percentage of sunspots in the Cortie classification corresponds to Type *I*, while in the Zürich classification it corresponds to Type *J*. The lowest percentage corresponds to Cortie Type *IIIb* and Zürich Type *B*, respectively. Sunspot groups that originally could not be associated with any of the Cortie types have been classified as NO DATA, and represent 0.3% of all observations. Sunspot groups that could not be converted to the Zürich classification (NO CONVERSION) represent 0.2% of all observations.

Table 3 shows a comparison of the percentages for the different Cortie types recorded at the observatories of Ebro and Kodaikanal (Ananthakrishnan, 1952) for the same period (1910–1937) and at the Valencia Observatory in the period 1920–1928 (Carrasco et al., 2015). For all three observatories, the higher percentages are obtained for Type *I* and *IV*. All the observed discrepancies, especially in Types *II*, *III*, and *V*, may be attributed to the bias from different observers (Carrasco et al., 2015), but also may be down to the fact we consider different periods.

We have done a similar study considering the Zürich classification. Table 4 shows a comparison of the percentages for the different Zürich types recorded at different periods of time at the Ebro, Madrid (Lefèvre et al., 2016), Valencia (Carrasco et al., 2015) and Ondřejov

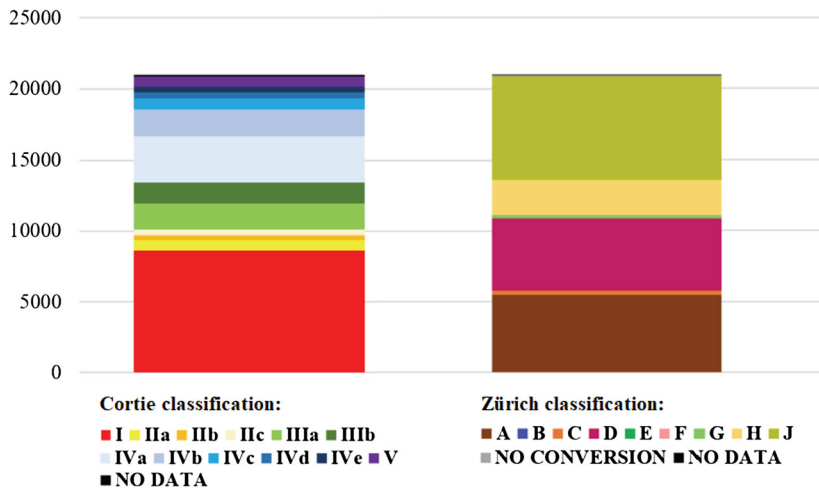


**Figure 1** Distribution of the sunspot groups occurrences recorded at the Ebro Observatory in the period 1910–1937 according to the Cortie and Zürich classifications. NO DATA (0.3%) represents group cases without classification and NO CONVERSION (0.2%) represents group cases in the Cortie classification that cannot be converted. The percentages for the different types in the Cortie classification are: I (41.3%), IIa (3.2%), IIb (1.7%), IIc (2.1%), IIIa (8.8%), IIIb (6.9%), IVa (15.6%), IVb (9.1%), IVc (3.5%), IVd (1.9%), IVe (1.9%) and V (3.6%); in the Zürich classification are: A (25.9%), B (< 0.1%), C (1.4%), D (24.4%), E (0.1%), F (0.1%), G (1.0%), H (12.1%), and J (34.5%).

**Table 4** Percentages of the Zürich types at the Ebro Observatory (this study), Madrid Observatory (Lefèvre et al., 2016), Valencia Observatory (Carrasco et al., 2015), Ondřejov Observatory (Kleczek, 1953) and the USET catalogue (Carrasco et al., 2015) in different periods.

Zürich type	Ebro (1910–1937)	Madrid (1914–1920)	Valencia (1920–1928)	Ondřejov (1938–1950)	USET (1940–2014)
A	26.1%	23.7%	19.3%	28.7%	18.9%
B	< 0.1%	2.3%	7.2%	11.2%	14.4%
C	1.4%	4.7%	11.3%	12.3%	17.8%
D	24.5%	14.4%	18.1%	11.1%	15.6%
E	0.1%	5.0%	7.3%	7.6%	4.8%
F	0.1%	2.0%	4.6%	2.0%	1.3%
G	1.0%	0.9%	2.2%	5.1%	2.7%
H	12.1%	6.4%	7.7%	8.0%	5.3%
J	34.7%	40.6%	22.3%	13.8%	19.2%

(Kleczek, 1953) observatories. For all sets of data, the higher percentage types are obtained for A, D, and J. In comparison with the rest of observatories, the Ebro data present much lower values of Types B, C, E and F and a slight excess of Type H. This may be due to the initial percentages in the Cortie classification that lead through the conversion to certain types in the Zürich classification. It should also be remembered that we are comparing data from different periods of time.

Figure 2 presents the distribution of the average areas of the sunspot groups using both the Cortie and the Zürich classifications of the Ebro Observatory data registered in the period

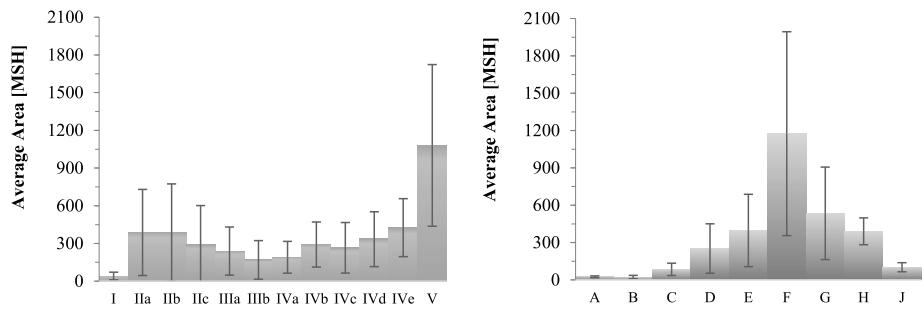


**Figure 2** Average area of the sunspot groups in the Cortie and Zürich classifications obtained from the Ebro Observatory data in the period 1910–1937.

1910–1937. The distribution obtained for the Cortie classification is very close to the results for the Valencia and Madrid observatories (Carrasco et al., 2015; Lefèvre et al., 2016). In the case of the Zürich classification, the distribution is also quite similar to the Valencia results (Carrasco et al., 2015), and it also matches data from the Royal Greenwich Observatory (RGO) and the US Air Force (USAF) catalogues (Lefèvre and Clette, 2011; Kilcik et al., 2011, 2014).

### 2.3. Solar Plage Classification

Over time, solar plage groups have also been classified by using different criteria and several methodologies. In contrast to the study of sunspots, a unified classification has not yet been established. Examples of these methods include the one proposed by Righini and Godoli (1950), based on the character figures of the solar phenomena, a numeric scale from 0 to 5, which the solar plagues are associated with according to their abundance and intensity on the solar disc; or the one suggested by Kobel et al. (2009), who used a statistical classification approach based on Linear Discriminant Analysis applied to their data, with the aim of looking for patterns and defining features. For its part, the Ebro Observatory established its own classification (Cirera, 1910), composed initially of 3 different types of solar plagues, arranged according to their shape and dissemination (Table 5). However, in 1920 the Ebro Observatory transferred the direction of the centre from Fr. R. Cirera to Fr. L. Rodés, who extended this classification method adding an extra type, the *diffuse class*, composed of those solar plagues that could not be associated easily to any initial group because of the low quality of the photographs or their irregular shape (Rodés, 1920; Curto et al., 2016).

A similar classification was adopted by the Madrid Observatory in the period 1912–1917, in which solar plagues were classified according to their condensation in four categories: (cc) very condensed, (c) condensed, (s) subdivided, and (ss) very subdivided. They judged whether the solar plagues were observed as a single, continuous, and compact surface or, on the contrary, whether the solar plagues appeared fragmented, in several grouped areas (Vaquero et al., 2007).

As with sunspot groups, we analysed the solar plage records of the Ebro Observatory in the period 1910–1937 and carried out a study of the percentage of each solar plage type and also the distribution of their average areas. It should be mentioned that due to the nebulous and ill-defined nature of the floccular particles within solar plage groups, the area measurements of these structures were made only of their global extent, without analysing the areas

**Table 5** Ebro Observatory classification of solar plages. The diffuse class was introduced in 1920 after the application of Rodés’ criteria.

<i>c</i>	Compact solar plages. They are presented together in a single mass without notable lacks of continuity or interruptions.
<i>d<sub>i</sub></i>	Scattered solar plages. They are divided into isolated parts with a certain area. The subscripts 1, 2, 3 specify 3 grades of scattering (minimum, medium and maximum, respectively), which indicates the quantity of floccular particles within the region which comprises them. The degree of scattering can be useful in the study of their formation, development and disappearance.
<i>cd</i>	Solar plages composed of <i>c</i> and <i>d</i> . They are defined as the transition state between <i>c</i> and <i>d</i> class
diffuse	Solar plages that cannot be associated to any group.

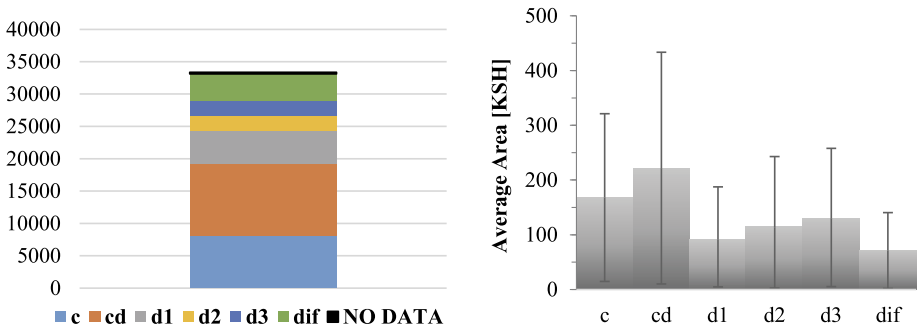


**Figure 3** Left panel: Distribution of the solar plage groups recorded at the Ebro Observatory in the period 1910–1937 according to the Ebro classification. NO DATA (0.7%) represents group cases without classification. The percentages for the different types are *c* (24.3%), *cd* (33.2%), *d<sub>1</sub>* (15.6%), *d<sub>2</sub>* (6.9%), *d<sub>3</sub>* (6.9%), *dif* (12.5%); Right panel: Average area of the solar plage groups obtained from the Ebro Observatory data in the period 1910–1937.

of the inner elements (Cirera, 1910). Figure 3 shows the main results. The highest percentage of solar plages corresponds to Type *cd*, while the lowest percentage corresponds to Type *d<sub>2</sub>*, closely followed by Type *d<sub>3</sub>*. Those solar plage groups with no information regarding their type have been classified as NO DATA and represents 0.7% of all the results.

The similarities in the criteria used in the classification schemes proposed by the Ebro and Madrid observatories make it possible to compare both data sets. Tables 6 and 7 show respectively the percentages for the different types recorded at the Ebro Observatory (1910–1937) and Madrid Observatory (1912–1917) (Vaquero et al., 2007), with each one under its own classification scheme. It can be seen that the sum of percentages associated to solar plage group types with higher compact level (*c*+*cd*) belonging to the Ebro Observatory is quite similar to their equivalent sum in the Madrid observatory (*cc*+*c*). The same occurs with those groups related to a high level of scattering or fragmentation (*d<sub>1</sub>*+*d<sub>2</sub>*+*d<sub>3</sub>*+*dif* and *s*+*ss*).

### 3. Analysis and Results

On the basis of Seguí et al. (2019) methodology, we studied the temporal variation of the sunspot and solar plage group types and areas in the period 1910–1937, and their associated N-S asymmetry. In particular, we examined both solar structures according to the types



**Table 6** Percentages of the different types of solar plages recorded at the Ebro Observatory (1910–1937).

Ebro classification (1910–1937)	
c	24.4%
cd	33.4%
d <sub>1</sub>	15.8%
d <sub>2</sub>	6.9%
d <sub>3</sub>	7.0%
dif	12.6%

**Table 7** Percentages of the different types of solar plages recorded at the Madrid Observatory (1912–1917) (Vaquero et al., 2007).

Madrid classification (1912–1917)	
cc	4.0%
c	50.0%
s	38.0%
ss	8.0%

within the different classification schemes, i.e., Cortie and Zürich for sunspot groups, and the Ebro Observatory classification for solar plages, by analysing the daily rate of occurrence and the annual distribution of each structure type (Section 3.1). In relation to the areas, we also studied their daily rate of occurrence and their annual distribution in accordance with four intervals of areas (Section 3.2). Finally, we examined the N-S asymmetry in all of the above features by doing an exhaustive statistical analysis (Section 3.3).

### 3.1. Occurrence Daily Rate and Distribution in Terms of the Classification Types

The evolution over time of sunspots and solar plage types can be studied in terms of the annual daily rate of occurrence as well as their annual distribution.

Despite having a temporal coverage close to 81% of the studied period (Figure 4), it is not possible to estimate the absolute occurrence daily rate due to the impossibility of achieving observational data for every day. The missing daily records may be due to weather conditions or technical problems. Hence, for every year of data, the relative average occurrence daily rate has been calculated as the ratio of the total number of observed occurrences of each type divided by the total number of observation days in this year. Moreover, the associated uncertainty has been computed as the standard deviation of the mean divided by the square root of the total number of observation days in the year.

As we noted in Seguí et al. (2019), the total occurrence daily rate of both sunspot and solar plage groups follows the habitual behaviour of solar cycles. This matches almost perfectly with the WDC-SILSO data corresponding to the sunspot number (<http://www.sidc.be/SILSO>), which place the different solar cycle minima in 1913, 1923 and 1933, and the solar cycle maxima in 1917, 1928, and 1937 (Figure 5, upper panel). In order to corroborate the resemblance between our series and WDC-SILSO data, a Pearson's correlation coefficient value of 0.986 for sunspot groups and 0.903 for solar plage groups have been found (Figure 5, lower panel). In addition, the Pearson's correlation coefficient between the total number of occurrences of sunspots and solar plages recorded at the Ebro Observatory has also been computed and has a value of 0.911.

Moreover, apart from the occurrence daily rate, the distribution of sunspots and solar plage types is also examined yearly within every classification scheme in terms of the per-

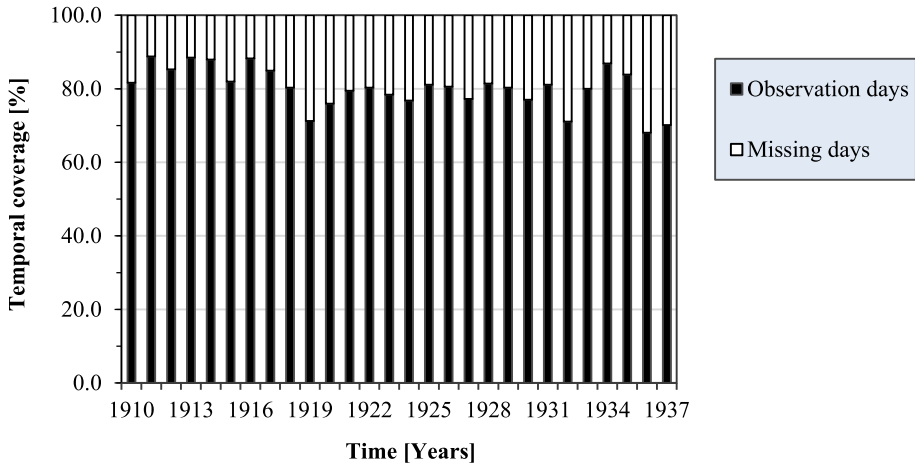


**Figure 4** Temporal evolution of the total number of observation days in the period 1910–1937. Results are expressed in percentages.

centage of each morphological type in relation to the total number of observations in the year.

### 3.1.1. Evolution of Sunspots According to Cortie Classification

Figure 6 shows the yearly evolution in the period 1910–1937 of the average occurrence daily rate of sunspot group types in the Cortie classification scheme, in conjunction with their associated average estimated by taking for each point of data  $i$ , the points  $i-2$ ,  $i-1$ ,  $i$ ,  $i+1$ , and  $i+2$ . It can be noted that the Cortie Types *I* and *IV* have the two highest occurrence daily rates in the whole period we studied, reaching values of  $2.6 \pm 0.2$  and  $2.0 \pm 0.1$  sunspot groups per day at the maximum of the 15th solar cycle respectively, presenting the same value of  $1.9 \pm 0.1$  sunspot groups per day at the maximum of the 16th solar cycle, and showing values of  $2.5 \pm 0.2$  and  $1.6 \pm 0.1$  sunspot groups per day at the maximum of the 17th solar cycle. In addition, it can be observed that the 17th solar cycle maximum has the highest total occurrence daily rate, with a value of  $6.2 \pm 0.4$  sunspot groups per day. By contrast, taking the years 1917 and 1928 as a reference of the maxima of the 15th and 16th solar cycles, it can be noted that they present a total value of  $6.0 \pm 0.3$  and  $4.8 \pm 0.3$  sunspot groups per day. This fact indicates that the 17th solar cycle presents a greater solar activity in the form of sunspots in its maximum. Nevertheless, the total number of observed occurrences is about 2% higher in the 16th cycle than in the 15th. This is a consequence of the Waldmeier effect (Waldmeier, 1955), i.e. the length of the 16th solar cycle is longer and it reaches the maximum faster, in contrast to the 15th cycle.

Figure 7 shows the temporal evolution of the annual distribution of the different types in the Cortie classification in terms of percentages of each type with respect to the total number of observations. It can be observed that Types *I* and *IV* are the most frequent in the whole period, with a mean value of  $(41 \pm 7)\%$  and  $(31 \pm 9)\%$ , respectively; they are followed by Type *III*, which is  $(16 \pm 6)\%$ . Types *II* and especially *V* are virtually marginal during all the period. Moreover, at the minimum of the 14th solar cycle, Type *II* reaches a value of 42%, at the same time as Type *IV* becomes temporally marginal. Nevertheless, this event occurs inside a solar cycle minimum, at the time that Type *II* presents an occurrence daily rate very

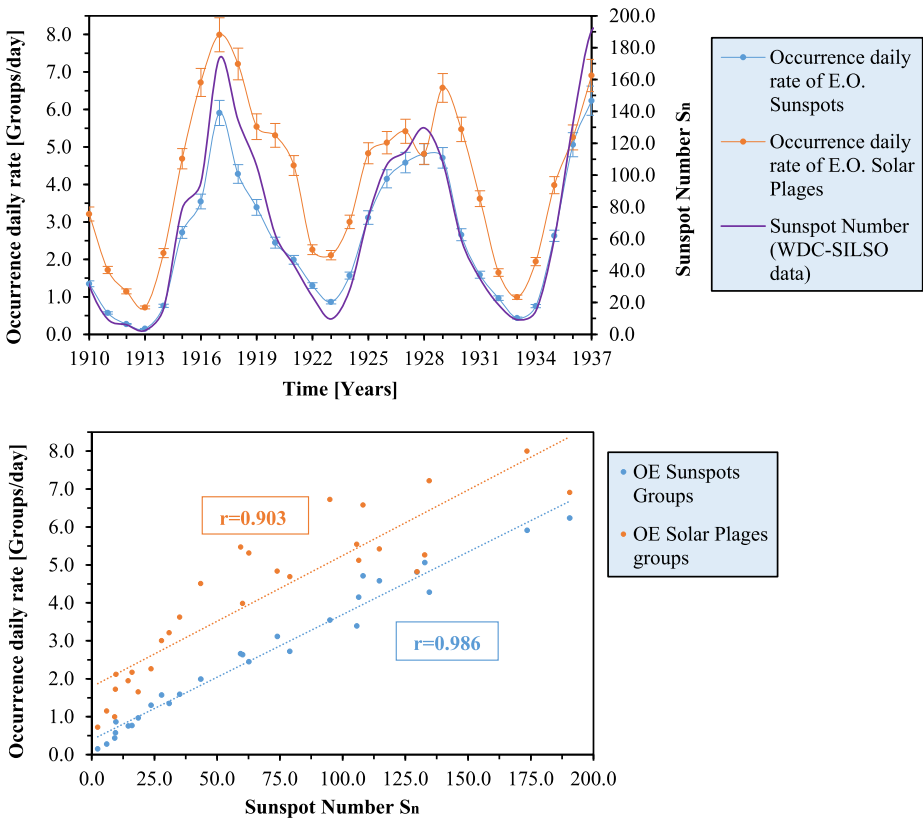


**Figure 5** Upper panel: Comparison between the yearly mean total sunspot number obtained from WDC-SILSO data in the period 1910–1937, and the yearly occurrence daily rate of all sunspot and solar plage groups recorded at the Ebro Observatory in the period 1910–1937. Lower panel: Correlation values between the occurrence daily rate of sunspot/solar plage groups and the Sunspot Number obtained from WDC-SILSO data.

close to 0. In addition, it should be noted that in the beginning of the 16th cycle, Type III increases by 13%, while Type IV decreases by the same percentage. Finally, in contrast to Type I, which presents a small decrease in percentage during all the studied period, Types II and III experience a clear decrease and increase, respectively, with time.

### 3.1.2. Evolution of Sunspots According to the Zürich Classification

Figure 8 shows the temporal evolution in the period 1910–1937 of the average occurrence daily rate of sunspot group types in the Zürich classification scheme, in conjunction with their associated average. It can be observed that in the whole period the most important Zürich types are the J, A and D ones, and they present the higher occurrence daily rates near the three solar cycle maxima under consideration, reaching values of  $2.5 \pm 0.1$ ,  $1.3 \pm 0.1$ , and  $1.1 \pm 0.1$  sunspot groups per day, respectively, around the 15th solar cycle maximum, a set of values of  $1.5 \pm 0.1$ ,  $1.4 \pm 0.1$ , and  $1.3 \pm 0.1$  sunspot groups per day around the 16th solar cycle maximum, and values of  $1.9 \pm 0.1$ ,  $1.4 \pm 0.1$ , and  $2.1 \pm 0.1$  sunspot groups per day around the maximum of the 17th solar cycle.

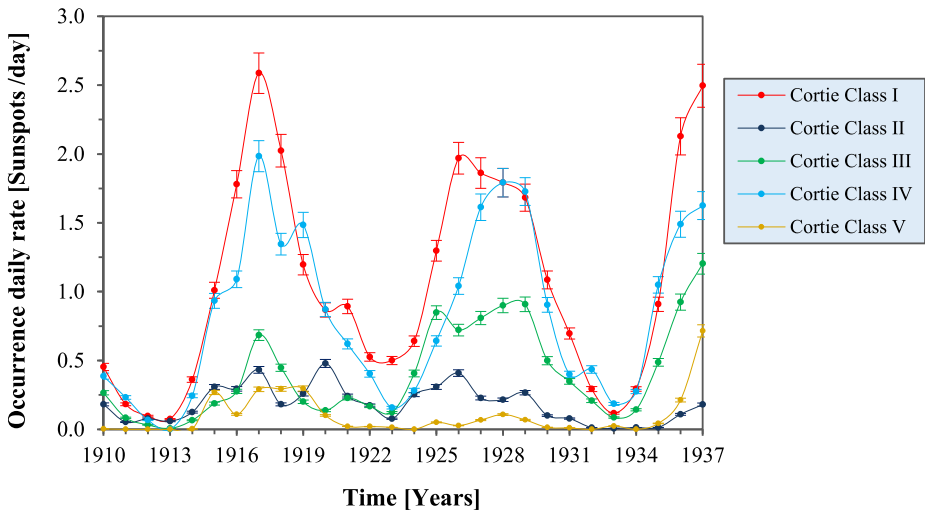


**Figure 6** Average occurrence daily rate of sunspot groups types in the Cortie classification in the period 1910–1937. The error bars show the standard deviation of the mean.

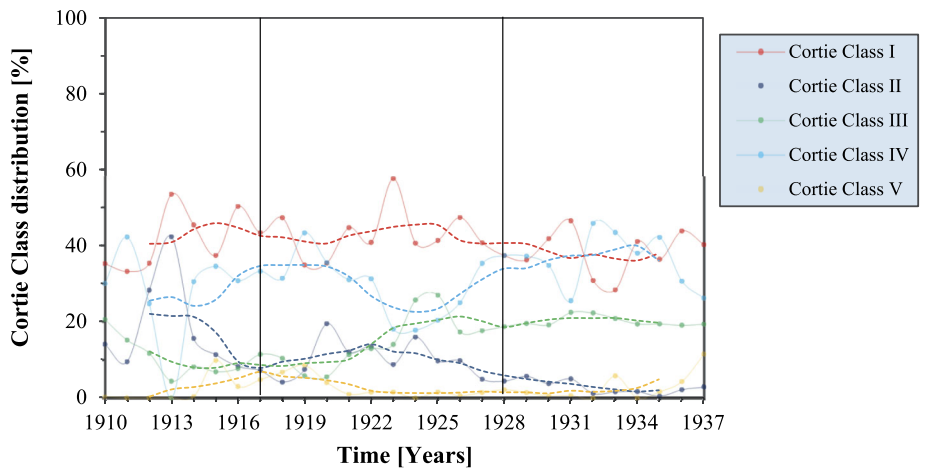


**Figure 7** Evolution over time of the distribution of types of sunspot groups in the Cortie classification. Solid lines show the temporal evolution of the annual distribution of the different types in the Cortie classification in terms of percentages of each type with respect to the total number of observations. Dashed lines show the smoothed data belonging to each type of sunspot group. The smoothing of the data plotted here and later in Figures 9, 11, 13, and 15 were done by considering for each year  $i$ , the average from the years  $i - 2, i - 1, i, i + 1$  and  $i + 2$ . Vertical solid lines in 1917, 1928 and 1937 represent the three solar maxima corresponding to the 15th, 16th, and 17th cycles.

In relation to the temporal evolution of the annual distribution of the different types of sunspots in the Zürich classification (Figure 9), it can be observed that Types  $J$ ,  $A$  and  $D$  are the most frequent in the whole studied period, with mean values of  $(34 \pm 7) \%$ ,  $(27 \pm 6) \%$ , and  $(25 \pm 5) \%$ , respectively; they are followed by Type  $H$ , which is  $(10 \pm 5) \%$ . Types  $C$ ,  $G$ , and especially  $B$ ,  $E$  and  $F$  are virtually marginal during all the period.

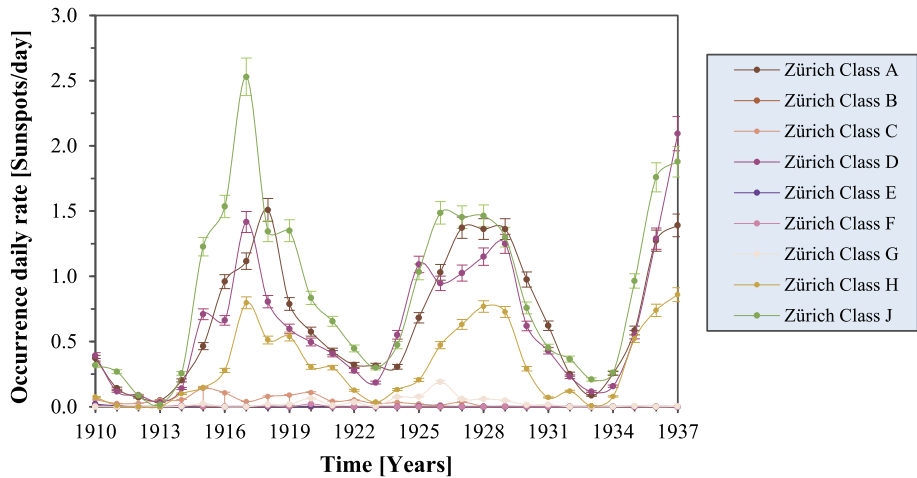


**Figure 8** Average occurrence daily rate of sunspot groups types in the Zürich classification in the period 1910–1937. The error bars show the standard deviation of the mean.

### 3.1.3. Evolution of Solar Plages According to Ebro Observatory Classification

Figure 10 shows the year by year evolution in the period 1910–1937 of the average occurrence daily rate of solar plage group types in the Ebro Observatory classification scheme. In the case of these chromospheric structures, the normal behaviour of the solar activity through the cycles is still preserved, and the shape of all curves is quite similar to those observed in all types of sunspot groups.

It can be observed that Type *cd* solar plage groups have the highest occurrence daily rate in practically all the period, reaching values of  $3.4 \pm 0.2$ ,  $1.6 \pm 0.1$  and  $1.9 \pm 0.2$  solar plage groups per day at the respective maxima of the 15th, 16th and 17th solar cycles. Nonetheless, these types of solar plages are followed closely by Types *c* and *d*, which reach a local maximum value of  $2.5 \pm 0.1$  and  $2.3 \pm 0.1$  solar plages per day respectively around the 15th solar cycle maximum,  $1.4 \pm 0.1$  and  $2.1 \pm 0.1$  solar plages per day in 1929, i.e., one year after the 16th solar cycle maximum, and  $1.7 \pm 0.1$  and  $1.9 \pm 0.1$  solar plages per day in the 17th solar cycle maximum.

The fact that solar plages tend to be more scattered and diffuse in the declining phase of practically each solar cycle is noteworthy while Types *c* and *cd* dominate at the beginning of the cycles (Seguí et al., 2019).

It also can be noted that the 15th solar cycle maximum has the highest total occurrence daily rate, with a value of  $8.0 \pm 0.5$  solar plages per day in 1917, i.e., one year before the solar maximum. By contrast, considering the years 1929 and 1937 as a reference for the maxima of the 16th and 17th solar cycles, values of  $6.5 \pm 0.4$  and  $6.9 \pm 0.4$  solar plages per day, respectively, can be observed. Thus, the 15th solar cycle presents a greater solar activity in the form of cases of solar plages in its maximum. In addition, despite the characteristic strongly peaked shape of the 15th solar cycle, its total number of observed occurrences is about 7% higher than in the 16th. This is because of the large amplitude of the *cd* and *d* profiles during the 15th solar cycle.

Regarding the temporal evolution of the annual distribution and average of the different types of solar plages in the Ebro Observatory classification (Figure 11), the most frequent morphology observed in the whole studied period is Type *cd*, with a mean value of

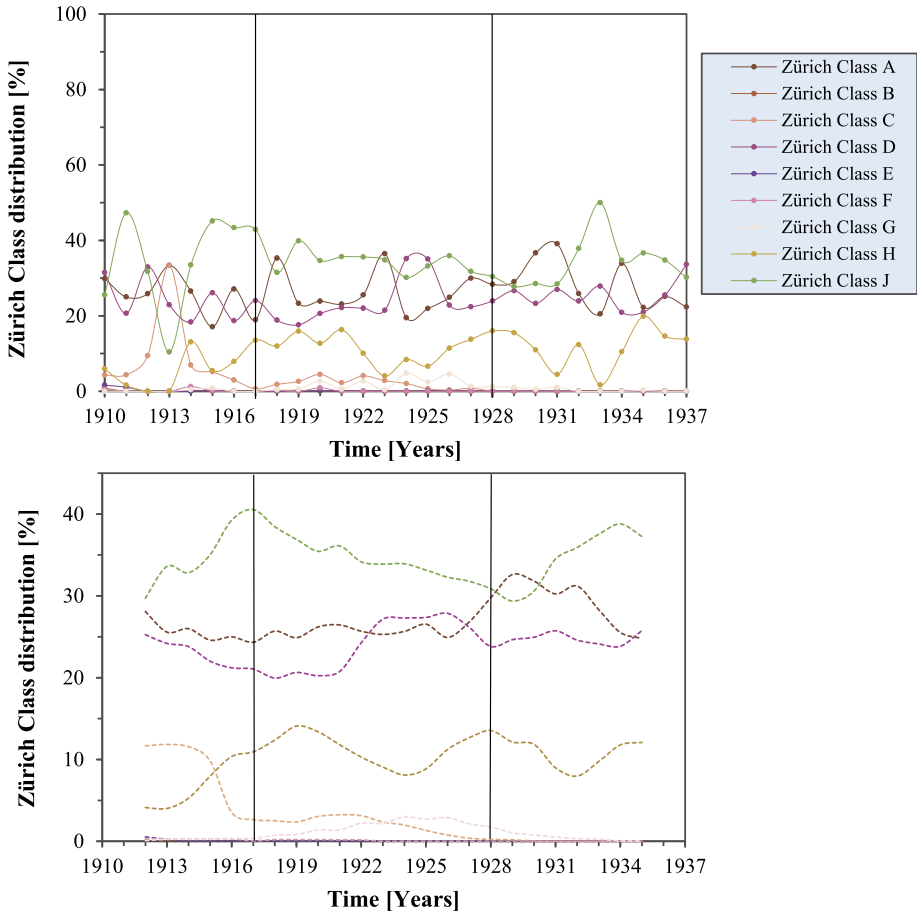


**Figure 9** Upper panel: Temporal evolution of the annual distribution of the different types in the Zürich classification in terms of percentages of each type with respect to the total number of observations. Lower panel: smoothed data corresponding to all types of sunspot groups. Vertical solid lines in 1917, 1928 and 1937 represent the three solar maxima corresponding to cycles 15th, 16th and 17th.

( $31 \pm 8$ ) %. It is closely followed by Type *d* ( $30 \pm 7$ ) % and Type *c* ( $26 \pm 8$ ) %. Moreover, since the classification was not extended to include the Diffuse option until 1920, this type is obviously absent from records for the first 9 years of the studied period, but from then on it begins to oscillate with a mean of ( $21 \pm 6$ ) %. Hence, the mean annual distribution of the rest of the types suffer a slight drop between 5.0–10.0% from 1920 onwards.

### 3.2. Occurrence Daily Rate and Distribution in Terms of Areas

The temporal evolution of sunspots and solar plage areas is studied in terms of the relative average occurrence daily rate as well as their annual distribution.

For both solar structures, we took four different bins of areas in which we classified all the observations. Then, for each area bin and year, we calculated the relative average occurrence daily rate as the ratio of the number of observed occurrences of each bin divided by the total

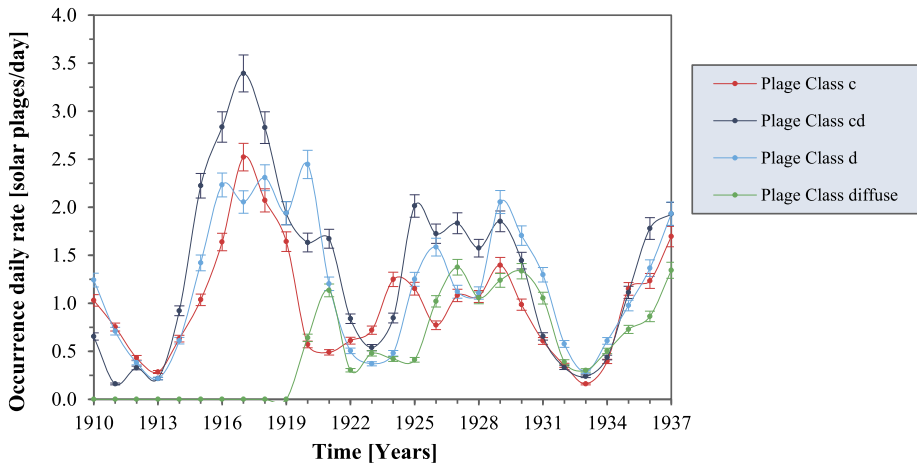


**Figure 10** Average occurrence daily rate of types of solar plage groups in the Ebro Observatory classification in the period 1910–1937. The error bars show the standard deviation of the mean.

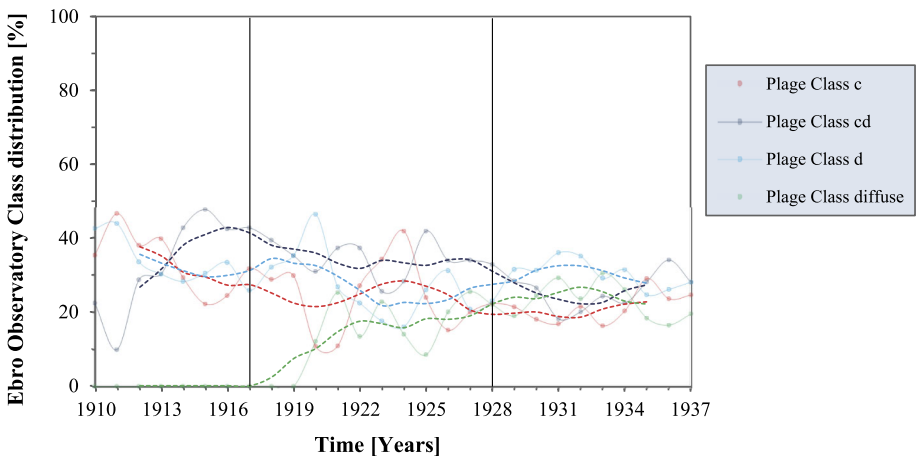


**Figure 11** Evolution over time of the distribution of types of solar plage groups in the Ebro Observatory classification. Solid lines show the temporal evolution of the annual distribution of the different types in terms of percentages of each type with respect to the total number of observations. Dashed lines are related to the smoothed data belonging to each type of solar plage group. Vertical solid lines in 1917, 1928 and 1937 represent the three solar maxima corresponding to cycles 15th, 16th and 17th.

number of observation days in the year. We also estimated the associated uncertainty as the standard deviation of the mean divided by the square root of the total number of observation days in the year. The annual distribution of sunspot and solar plage areas was also examined in terms of the percentage of each area bin from the total number of observations in the year. With the objective of better analyse the trends, we also computed the averages of all the distributions.

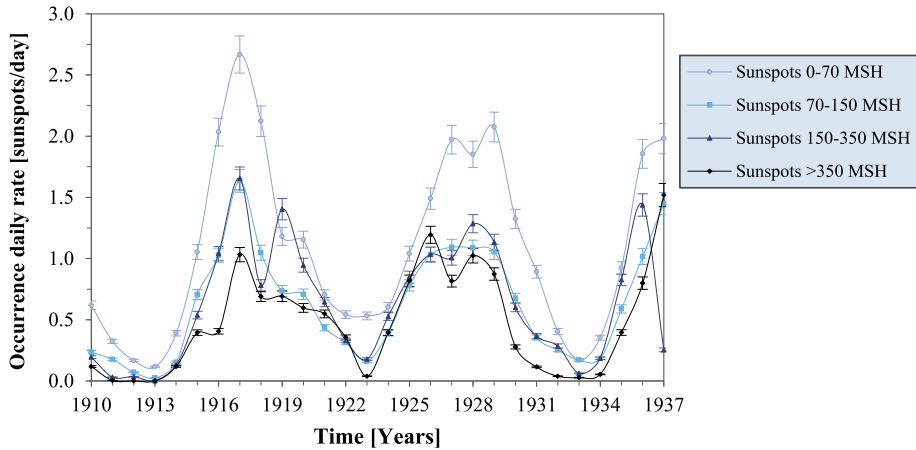


**Figure 12** Average occurrence daily rate of sunspot groups of a certain area (in MSH units) in the period 1910–1937. The error bars show the standard deviation of the mean.

### 3.2.1. Sunspot Areas

It can be observed that in the whole period under study, the occurrence daily rate (Figure 12) and the distribution (Figure 13) increase significantly as the area of sunspot groups decreases.

In particular, sunspot groups with areas of 0–70 MSH reach values of  $2.7 \pm 0.2$  occurrences per day at the maximum of the 15th solar cycle,  $2.1 \pm 0.1$  per day in 1929, and  $2.0 \pm 0.1$  per day at the maximum of the 17th solar cycle. Regarding the distribution, the smaller sunspots are more dominant than the rest, especially near the solar cycle minima (Figure 13), and they have a mean of  $(43 \pm 10)\%$  within all the studied period. This is consistent with the distribution in terms of the morphological classification since, as Figure 2 shows, all groups of Type *I* in the Cortie classification, or all groups of Type *A* and a small fraction of groups of Type *J* in the Zürich classification can be related with general sunspot groups of areas smaller than 70 MSH.

By contrast, sunspot groups with areas larger than 350 MSH are the least relevant in numbers, reaching occurrence rates of only  $1.0 \pm 0.1$  per day at the maximum of the 15th and 16th solar cycles, and  $1.5 \pm 0.1$  per day at the maximum of the 17th solar cycle. In terms of the distribution, the mean percentage of the largest sunspots is  $(14 \pm 8)\%$  and shrinks below 5% during the solar cycle minima.

### 3.2.2. Solar Plage Areas

It can be noted that for most of the studied period, the occurrence daily rate (Figure 14) and the annual distribution (Figure 15) increase significantly as the area of solar plage groups decreases. Nevertheless, this behaviour seems to be reversed completely at the beginning of the 16th and 17th solar cycles. Thus, solar plage groups with areas of 0–70 100 KSH reach occurrence rates of  $4.7 \pm 0.3$  per day near the maximum of the 15th solar cycle,  $3.0 \pm 0.2$  per day in 1930, i.e., two years after the maximum of the 16th solar cycle; and only  $0.7 \pm 0.1$  per day at the maximum of the 17th solar cycle.

Conversely, solar plage groups with areas of 150–350 100 KSH and larger than 350 100 KSH, reach occurrence rates of  $1.4 \pm 0.1$  and  $0.4 \pm 0.1$  per day at the maximum of the 15th



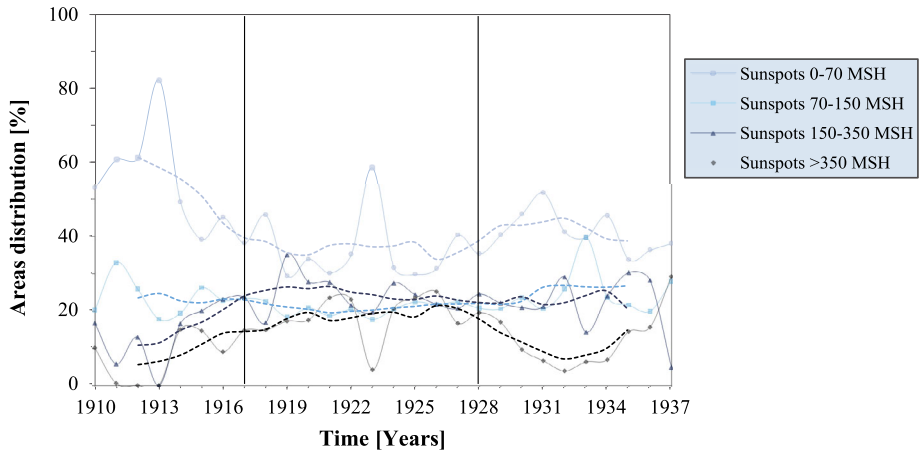


**Figure 13** Evolution over time of the distribution of sunspot groups of a certain area (in MSH units). Solid lines show the temporal evolution of the annual distribution of sunspot groups for each area bin. Dashed lines are related to the smoothed data corresponding to each area bin. Vertical solid lines in 1917, 1928 and 1937 represent the three solar maxima corresponding to cycles 15th, 16th and 17th.

solar cycle, and rapidly increase their values to  $2.1 \pm 0.1$  and  $1.1 \pm 0.1$  solar plages/day in 1920, at the same time as the smallest groups present an occurrence rate of only  $0.7 \pm 0.1$  per day. One year after the 16th solar cycle maximum, the largest groups achieve values of  $1.5 \pm 0.1$  and  $0.9 \pm 0.1$  solar plages/day, respectively. And finally, in the 17th solar cycle maximum they reach occurrence rates of  $2.3 \pm 0.1$  and  $2.1 \pm 0.1$  per day.

Regarding the area distribution, with a mean of  $(42 \pm 20)\%$ , the smallest solar plages are dominant, especially near the solar cycle minima (Figure 15). By contrast, the mean percentage of the largest solar plages is  $(12 \pm 10)\%$  and shrinks below 5% in all solar cycle minima. Nevertheless, near the 16th maximum and especially the 17th, plage groups tend to increase their areas and became more numerous, and even predominant.

### 3.3. North–South Asymmetry

There are two primary ways to quantify the N-S asymmetry: through the absolute asymmetry index  $\Delta$  (Equation 3.3.1), and by using the relative (or normalized) asymmetry index  $\delta$  (Equation 3.3.2), where  $A_N$  and  $A_S$  represent the activity in the northern and southern hemisphere, respectively.

$$\Delta = A_N - A_S, \tag{3.3.1}$$

$$\delta = \frac{\Delta}{A_N + A_S} = \frac{A_N - A_S}{A_N + A_S}. \tag{3.3.2}$$

The normalized asymmetry index (Lefcus, 1960) is usually used since the absolute asymmetry presents very high values near the solar cycle maxima (Zhang, 2012). Nonetheless, it has been observed that the normalized asymmetry index presents values close to 1 near the solar cycle minima when most of the structures associated with the solar activity are formed in one of the two hemispheres. This effect is due to the low number of structures observed during a solar cycle minimum (Swinson, Koyama, and Saito, 1986; Vizoso and Ballester, 1990). In this work we computed the normalized N-S asymmetry index  $\delta$  of all

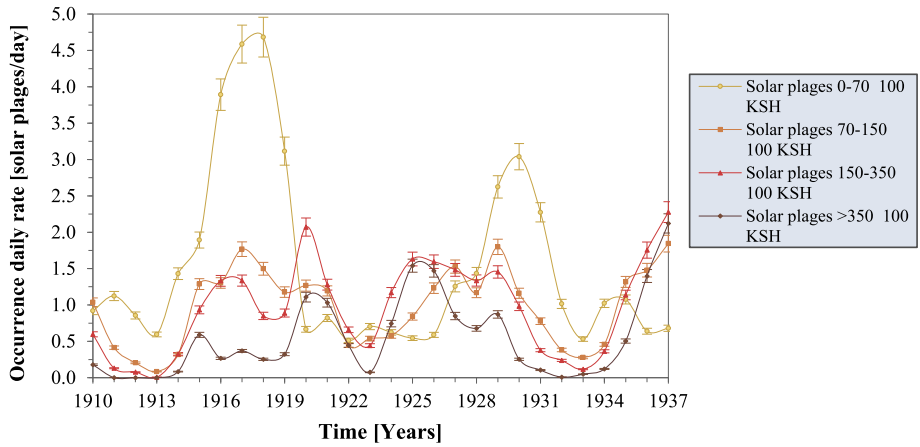


**Figure 14** Average occurrence daily rate of solar plage groups of a certain area (in 100 KSH units) in the period 1910–1937. The error bars show the standard deviation of the mean.

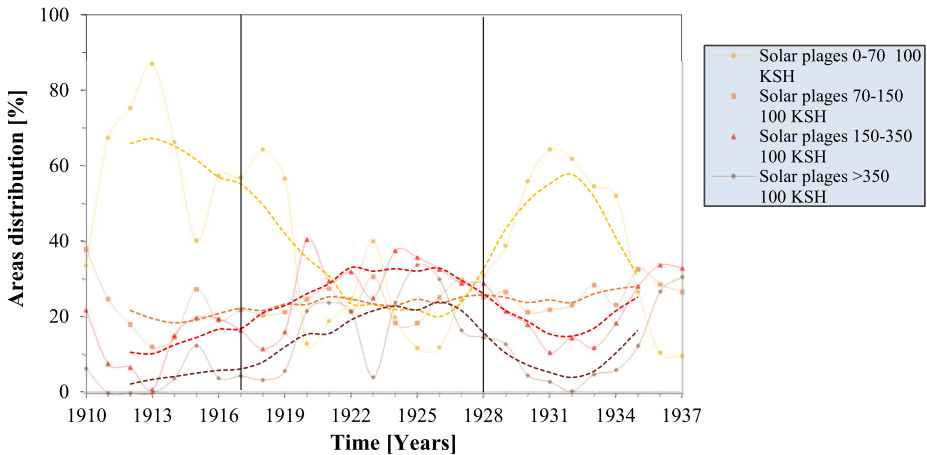


**Figure 15** Evolution over time of the distribution of solar plage groups of a certain area (in 100 KSH units). Solid lines show the temporal evolution of the annual distribution of solar plage groups for each area bin. Dashed lines are related to the smoothed data corresponding to each area bin. Vertical solid lines in 1917, 1928 and 1937 represent the three solar maxima corresponding to cycles 15th, 16th and 17th.

the features presented in Sections 3.1 and 3.2 related to sunspot and solar plage groups. We also compared our normalized N-S asymmetry index  $\delta$  values with those obtained by using the RGO data in the studied period, available in the Solar Physics website of the NASA Marshall Space Flight Center (<https://solarscience.msfc.nasa.gov/greenwch.shtml>).

In order to check the statistical significance of the normalized N-S asymmetry index values, in addition to the Letfus formula (Equation 3.3.3), we based our work on the method used by Wilson (1987) to study the east–west asymmetry of solar flares. First of all, for sunspots and solar plage groups, we verified the asymmetry in terms of the excess,  $E$ , which is a measure of the significance of the difference,  $d$ , in the number of structures in each hemisphere in a certain period of time. The excess is calculated according to Equation 3.3.4,

where  $n$  is the total number of occurrences in that period of time.

$$SS_{\delta} = \pm [2(A_N + A_S)]^{-1/2}, \tag{3.3.3}$$

$$E = d \left(\frac{n}{2}\right)^{-\frac{1}{2}}. \tag{3.3.4}$$

Then, we computed the probability of obtaining the observed results or having a larger difference due to randomness,  $P(\geq d)$ , which is derived from the binomial distribution formula that describes the probability of obtaining a distribution of  $n$  objects in two classes:

$$P(k) = \binom{n}{k} p^k (1-p)^{n-k} = \frac{n!}{k!(n-k)!} p^k (1-p)^{n-k} \tag{3.3.5}$$

where  $n$  is the total number of objects,  $k$  is the number of objects in one class, and  $p$  is the success probability associated to that class (in our case  $p = 1/2$ ). Then, the probability is given by Equation 3.3.6:

$$P(\geq d) = \sum_{i=d}^n P(i). \tag{3.3.6}$$

Generally, when  $E < 2$  and  $P(\geq d) > 10\%$ , it denotes an insignificant result. If  $2 \leq E < 3$  and  $5\% < P(\geq d) \leq 10\%$ , it denotes a marginally significant result. The result is statistically significant when  $3 \leq E < 4$  and  $1\% \leq P(\geq d) \leq 5\%$ . Finally, a set of values of  $E \geq 4$  and  $P(\geq d) < 1\%$  indicates a highly significant result (Wilson, 1987).

### 3.3.1. N-S Asymmetry in the Total Number of Occurrences

Table 8 shows the computed values of  $E$ , the excess, and the probability of the normalized N-S asymmetry index observed in Figure 16, related to the total number of occurrences in both structures, without being grouped into any morphological type. The values reflect the fact that the asymmetry is highly significant in a great part of the studied period, and especially in the northern hemisphere, where the numbers are larger and the dominance is longer in time in comparison with the southern hemisphere. Moreover, only those years involved in the change of the preferred hemisphere present lower levels of asymmetry and excess.

The evolution over time of the normalized N-S asymmetry index is quite similar for both solar structures, but not equal. For all data sets, three remarkable maxima can be noted: in 1912 (southern hemisphere), and 1924 and 1933 (northern hemisphere); that is, in the minimum of each solar cycle, when  $\delta \geq 0.5$ ,  $E > 10$  and  $P(\geq d) \leq 1\%$ . But in contrast to the two data series of sunspots, solar plages present lower values of asymmetry in both hemispheres in practically all the period under consideration.

Finally, the comparison of the results with the Greenwich N-S asymmetry data puts ours to the test in a positive way, after obtaining a quite similar trend, with a Pearson’s correlation coefficient of 0.987 in the case of sunspots and 0.962 for solar plages. In fact, our results are in consonance with other N-S asymmetry studies in sunspots, faculae, and solar plages, such as Newton and Milsom (1955), Verma (1992) or Mandal et al. (2017), Mandal, Chatterjee, and Bajerne (2017), which also found a global predominance in the southern hemisphere in the 15th solar cycle and in the northern hemisphere in the 16th and 17th solar cycles. Moreover, the Pearson’s correlation coefficient between our sunspot and solar plage data presents a value of 0.949.

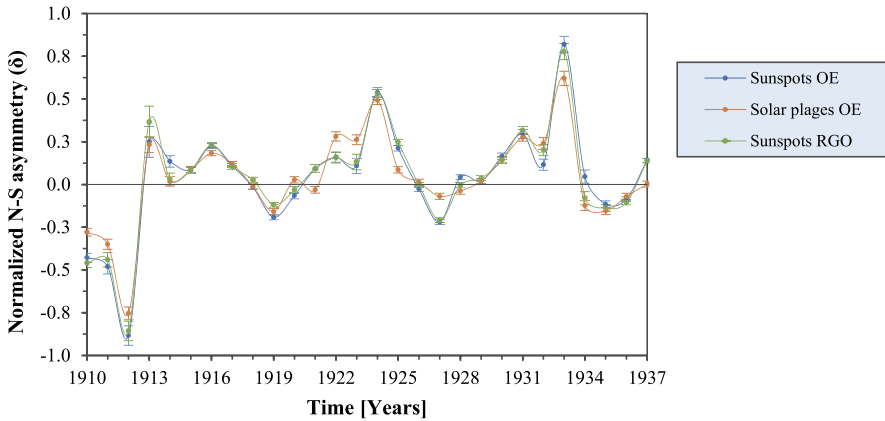


**Figure 16** Evolution over time of the normalized N-S asymmetry index in the period 1910–1937 in sunspots and solar plage group occurrences. The orange line represents the solar plage asymmetry, and the blue and green lines, the sunspot asymmetry for the OE and RGO data, respectively.

### 3.3.2. Morphological Types N-S Asymmetry

Figure 17 shows the temporal evolution of the normalized N-S asymmetry index and the correspondent uncertainty of sunspot group types in the Cortie classification, calculated by using the expressions 3.3.2 and 3.3.3, respectively. All groups present approximately the same trend observed in Figure 16, especially the most numerous kinds (Types *I*, *III* and *IV*), so it can be interpreted that the sunspot group type does not affect the asymmetry; or at least for our observation period. Erratic extreme asymmetry values can be observed for less frequent groups (Type *II*, and especially Type *V*). This behaviour is due to the low number of occurrences of these types, which causes strong changes in asymmetry, so it should be considered as not relevant.

After checking the significance of the results, we found that the asymmetry is significant toward the south during the declining phase of the 14th solar cycle, and highly significant in 1912, especially for Types *I* and *IV*. Moreover, the noteworthy extremes in 1924 and 1933 that the asymmetry presents in the northern hemisphere in Figure 16 can also be observed in Figure 17, especially for the sunspot groups of Type *IV*. Finally, two additional extremes of  $\delta > 0.5$  in 1921 and 1923 in Type *III* sunspot groups can also be observed. Just as the northern peak presents values of  $E = 6.3$  and  $P(\geq d) = 7\%$ , which is nearly close to a significant result, the southern one is statistically not significant ( $E = 4.5$  but  $P(\geq d) > 10\%$ ).

In the case of the Zürich classification (Figure 18), the most frequent classes (Types *J*, *A* and *D*) also follow the general trend of sunspots observed in Figures 16 and 17, and the characteristic extremes located at the solar cycle minima of the studied period are still appearing. Again, erratic extreme asymmetry values can be observed for the less frequent groups.

Focusing on the significance of the results, the southern peak in 1912 is highly significant for the *A* and *J* Types, and significant for the *C* and *D* ones. In the case of the 1924 northern maximum, the results show that it is highly significant for the *D* and *H* Types, and significant for the *A* and *J* ones. Moreover, the northern peak in 1933, is highly significant for Type *J*, significant for Type *D* and almost significant for Type *A* ( $E = 4.2$  and

**Table 8** Significance of the N-S asymmetry shown in Figure 16. The excess, *E*, and the probability of the asymmetry emerging by chance are shown, indicating a N or S hemisphere dominance. Marginal and non-significant periods are indicated in italics.

Year	Sunspots (OE)		Sunspots (RGO)		Solar plages (OE)	
	<i>E</i>	<i>P</i> (≥ <i>d</i> )	<i>E</i>	<i>P</i> (≥ <i>d</i> )	<i>E</i>	<i>P</i> (≥ <i>d</i> )
1910	12.1S	<1%	18.0S	<1%	12.2S	<1%
1911	9.3S	5%	10.4S	<1%	11.7S	<1%
1912	11.6S	<1%	15.0S	<1%	20.2S	<1%
1913	2.4N	5%	4.0N	2%	5.0N	<1%
1914	3.0N	1%	<i>0.9N</i>	<i>6%</i>	<i>0.6N</i>	<i>5%</i>
1915	3.4N	<1%	5.0N	<1%	4.5N	<1%
1916	10.8N	<1%	15.6N	<1%	12.0N	<1%
1917	6.6N	<1%	8.5N	<1%	8.5N	<1%
1918	<i>0.8S</i>	<i>4%</i>	<i>2.0N</i>	<i>1%</i>	<i>0.7S</i>	<i>3%</i>
1919	8.1S	<1%	8.0S	<1%	8.5S	<1%
1920	<i>2.4S</i>	<i>1%</i>	<i>1.7S</i>	<i>2%</i>	<i>1.5N</i>	<i>2%</i>
1921	3.1N	<1%	4.0N	<1%	<i>1.6S</i>	<i>2%</i>
1922	4.4N	<1%	5.2N	<1%	10.2N	<1%
1923	<i>2.4N</i>	<i>2%</i>	<i>2.9N</i>	<i>1%</i>	9.1N	<1%
1924	16.0N	1%	18.2N	1%	20.2N	1%
1925	9.1N	<1%	14.5N	<1%	4.6N	<1%
1926	<i>1.3S</i>	<i>3%</i>	<i>0.1S</i>	<i>3%</i>	<i>0.7N</i>	<i>4%</i>
1927	11.2S	<1%	14.4S	<1%	3.8S	<1%
1928	<i>2.3N</i>	<i>1%</i>	<i>0.3S</i>	<i>3%</i>	<i>2.1S</i>	<i>2%</i>
1929	<i>1.1N</i>	<i>3%</i>	2.6N	<1%	<i>1.2N</i>	<i>3%</i>
1930	6.4N	<1%	7.4N	<1%	8.0N	<1%
1931	9.1N	<1%	12.5N	<1%	12.7N	<1%
1932	<i>2.6N</i>	<i>2%</i>	6.2N	<1%	7.0N	<1%
1933	12.8N	<1%	16.5N	<1%	14.9N	<1%
1934	<i>1.0N</i>	<i>8%</i>	<i>2.1S</i>	<i>3%</i>	4.3S	<1%
1935	4.6S	<1%	7.0S	<1%	7.7S	<1%
1936	4.3S	<1%	7.8S	<1%	3.6S	<1%
1937	8.1N	<1%	11.9N	<1%	<i>0.1N</i>	<i>4%</i>

$P(\geq d) = 8\%$ ). By contrast, the northern extreme which Type *D* presents in 1913 is not significant since  $E = 2.1$  and  $P(\geq d) > 10\%$ .

The different morphological types of solar plage groups proposed by the Ebro Observatory also present a N-S asymmetry, and Figure 19 shows their evolution over time for the studied period. As with sunspots, all solar plage type groups follow approximately their global trend observed in Figure 16, including the three maxima, so it can be stated again that the morphology of these solar structures seems to have little effect on the normalized N-S asymmetry index.

The significance of the results verifies the previous statements. Therefore, the southern peak of 1912 is highly significant for all types of solar plages, except for the *diffuse* Type since there are no records for this type up to 1920 as we have explained previously. In the case of the northern maxima (1924 and 1933), they are highly significant for most of

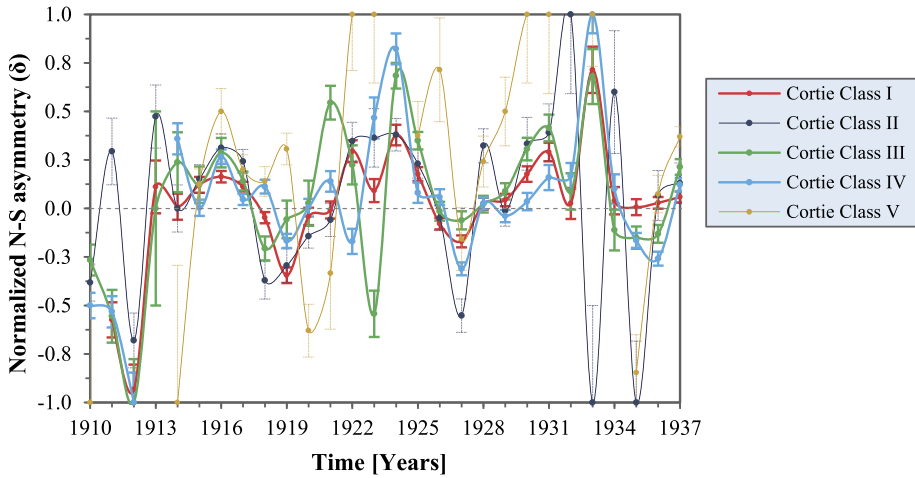


**Figure 17** Evolution over time of the normalized N-S asymmetry index in the period 1910–1937 in sunspot occurrences grouped in the Cortie classification. All the data correspond to the Ebro Observatory. Dashed lines indicate that the group has too few occurrences and may show extreme values.

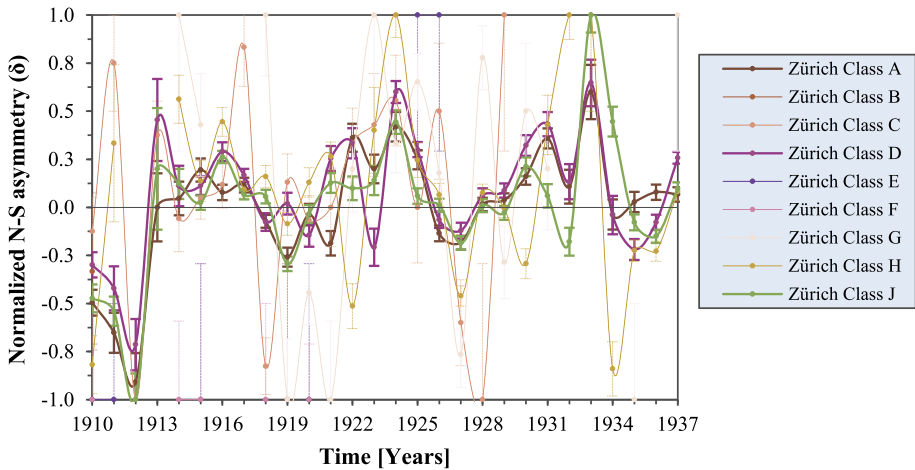


**Figure 18** Evolution over time of the normalized N-S asymmetry index in the period 1910–1937 in sunspot occurrences grouped in the Zürich classification. All the data correspond to the Ebro Observatory. Dashed lines indicate that the group has too few occurrences and may show extreme values.

the types. Only the cases of 1924-*d* class or Type, 1933-*d* Type and 1933-*diffuse* Type are significant, and present values of  $E \geq 7.1$  and  $P(\geq d) = 5\%$ . Furthermore, the northern peak in 1913 is only significant for Type *d* ( $E = 4.4$  and  $P(\geq d) = 1\%$ ).

### 3.3.3. N-S Asymmetry in Areas

Figures 20 and 21 show the temporal evolution of the normalized N-S asymmetry index and the correspondent uncertainty of sunspot groups divided in four different intervals of areas

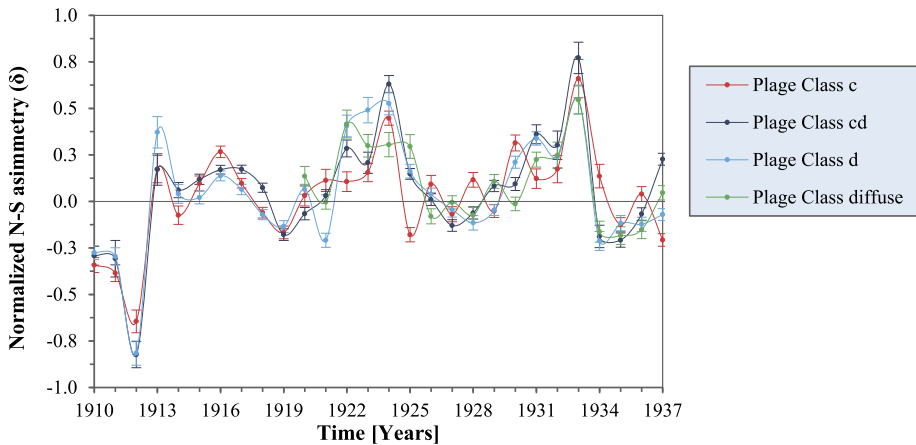


**Figure 19** Evolution over time of the normalized N-S asymmetry index in the period 1910–1937 in solar plage occurrences grouped in the Ebro Observatory classification. All the data correspond to the Ebro Observatory.

by using the Ebro Observatory and the RGO data, respectively. Once again, all the results are quite similar in comparison with the general evolution observed in Figure 16, but a slight dependence on area can be noted, in the sense that sunspot groups with larger areas present a stronger asymmetry.

With respect to the southern extreme of 1912, as well as the northern extremes of 1924 and 1933, present in practically all the area bins, they are significant or highly significant in most of the cases and for the two sets of data. However, in 1912 there is no data available for sunspot groups larger than 350 MSH at the Ebro Observatory, and the RGO data show that the asymmetry is not significant since there are only 5 observed occurrences in the southern hemisphere in their records ( $E = 3.2$  but  $P(\geq d) > 10\%$ ). Moreover, in 1933, the asymmetry for sunspot groups with areas up to 70 MSH is marginally significant towards the north with the RGO data ( $E = 7.0$  but  $P(\geq d) = 8\%$ ).

Furthermore, the normalized N-S asymmetry index in sunspot group areas shows some additional extremes in its temporal evolution. Thus, the fact that a northern maximum of  $\delta \sim 0.7$  can be located in 1914 for sunspot groups larger than 350 MSH is widely significant ( $E = 5.5$  and  $P(\geq d) = 4\%$ ) for the Ebro Observatory data and highly significant for the RGO records. In a similar way, three extra southern extremes can be observed in both sets of data in 1920, 1927 and 1934, especially for sunspot groups with areas larger than 350 MSH, which present values of  $\delta < -0.4$ . For this area bin, all the mentioned extremes are highly significant in both sets of records, with the exception of the 1920 maximum, which shows significant results at both observatories ( $E_{OE} = 9.7$  and  $E_{RGO} = 8.1$  and  $P(\geq d) = 5\%$  for both data sets).

In the case of solar plages, the normalized N-S asymmetry index also presents a subtle dependence on the area, since larger solar plage groups present higher values of asymmetry (Figure 22). Nevertheless, the evolution over time of the four intervals of areas is fairly close to the global trend observed in Figure 16. Hence, the extremes located in and around the solar cycle minima are highly significant in practically all the intervals of areas. Nonetheless, the largest structures are absent in the 1912 maximum, and in 1932 present no significant results ( $E = 2.0$  and  $P(\geq d) > 10\%$ ), since there are only two occurrences in the records.

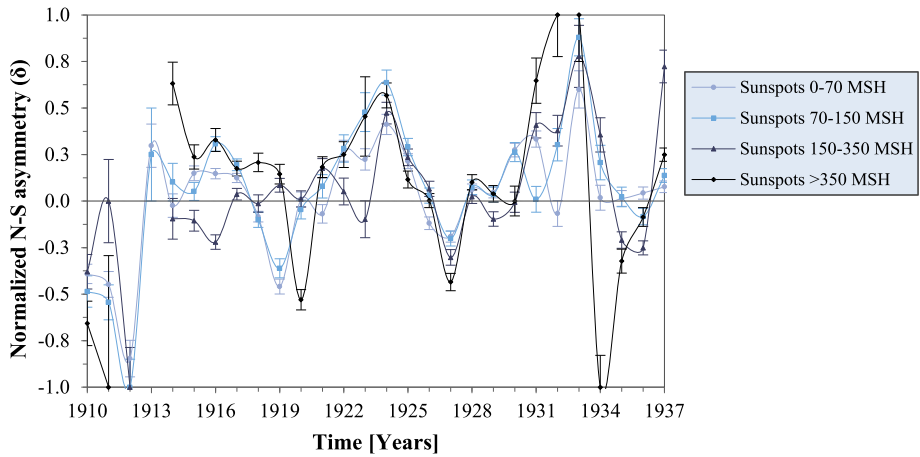


**Figure 20** Evolution over time of the normalized N-S asymmetry index in the period 1910–1937 in sunspot occurrences grouped in four area bins. All the data correspond to the Ebro Observatory.

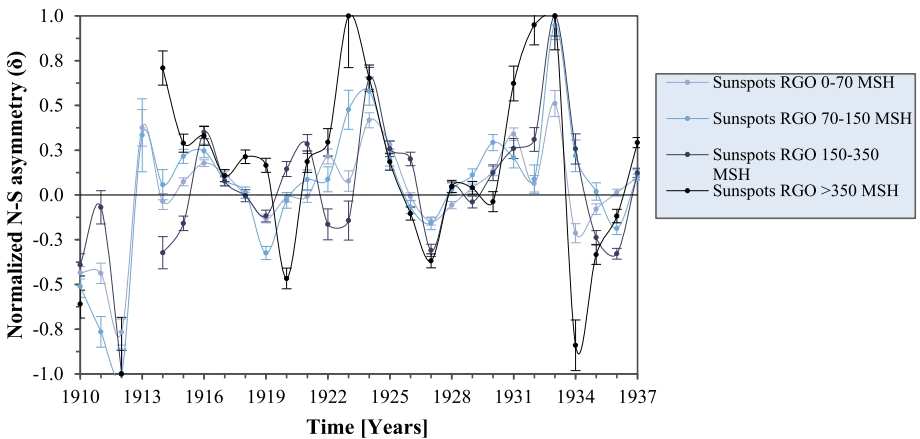


**Figure 21** Evolution over time of the normalized N-S asymmetry index in the period 1910–1937 in sunspot occurrences grouped in four area bins. All the data correspond to the RGO.

Finally, the normalized N-S asymmetry index in solar plage group areas also shows some additional extremes in its temporal evolution. The northern maximum located in 1913 for groups with areas of 150–350 100 KSH is not significant ( $\delta \sim 1.0$ ,  $E = 2.0$  and  $P(\geq d) > 10\%$ ) but it is highly significant for groups smaller than 70 100 KSH ( $\delta \sim 0.3$ ,  $E = 6.1$  and  $P(\geq d) < 1\%$ ). Likewise, the northern peaks of  $\delta > 0.6$  in 1914 and 1916 for solar plages larger than 350 100 KSH are significant since the excess and probability values are  $E = 5.2$  and  $P(\geq d) = 2\%$ , and  $E = 7.9$  and  $P(\geq d) = 1\%$ , respectively. In a similar way, an extra significant southern maximum can be observed in 1925 for the smallest groups, which presents values of  $\delta < -0.5$ ,  $E = 8.1$  and  $P(\geq d) = 3\%$ .



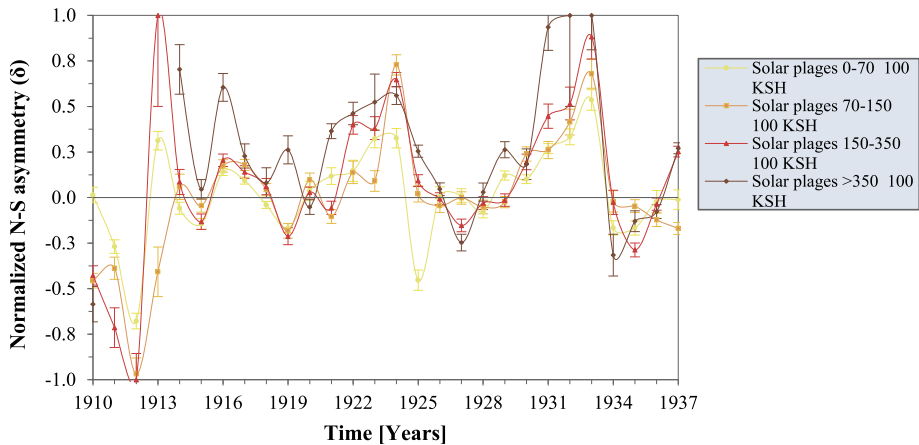


**Figure 22** Evolution over time of the normalized N-S asymmetry index in the period 1910–1937 in solar plage occurrences grouped in four area bins. All the data correspond to the Ebro Observatory.

#### 4. Discussion

With 81% of temporal coverage, the historical daily observations of sunspots and solar plage groups by the Ebro Observatory in the period 1910–1937 can contribute to broadening the knowledge of the general behaviour of these structures in a more detailed level and their variation over time, at least throughout the solar cycles under consideration. This work has focused on analysing, firstly, the global temporal evolution of the daily rate of occurrences and the distribution of both solar features according to the different morphological types and four area bins. After that, both hemispheres were considered separately in order to study the N-S asymmetry of the mentioned properties.

The yearly mean total sunspot number obtained from the recognized database of WDC-SILSO (<http://www.sidc.be/SILSO>) corroborates and strengthens our results in general terms. Hence, both sunspots and solar plage groups follow the general trend observed in the WDC-SILSO sunspot number, since our normalized calculations regarding the yearly occurrence daily rate of the total number of these structures, present Pearson's correlation coefficients of 0.986 and 0.903 respectively between their values and WDC-SILSO data. In addition, the Pearson's correlation coefficient between our sunspot and solar plage data shows a value of 0.911.

The morphology of sunspot groups was analysed according to the Cortie classification, but also in accordance with the Zürich scheme. In order to convert the original Cortie sunspot records into the Zürich classification, the equivalence criteria between both classification schemes proposed by Carrasco et al. (2015) was employed. In the period 1910–1937, sunspot groups tend to occur mostly in the form of Types *I*, *IV* in the Cortie classification, especially during the solar cycle maximum of each cycle. Similar conclusions can be extracted from the work of Ananthkrishnan (1952) and Carrasco et al. (2015) by examining the general distribution of sunspot records in the Cortie classification from the Kodaikanal and Valencia observatories in the periods 1910–1937 and 1920–1928, respectively. It is important to remark that all our results obtained with the Zürich classification, which show Types *J*, *A* and *D* in greater proportion in all the studied period, are compatible with the ones derived from the Cortie scheme, since the main morphological types of sunspot groups consist of small spots with or without penumbra (Types *I/J*, *A*) and bipolar groups whose

main spot has penumbra (Types *IV/D*). Akin distributions in the Zürich classification were also found by Carrasco et al. (2015) and Lefèvre et al. (2016) in the Valencia and Madrid observatories sunspot records in the periods 1920–1928 and 1914–1920, respectively. Moreover, all these results are comparable with those obtained by Oh and Chang (2012), who extracted analogous conclusions by studying the time variations of the monthly mean number of sunspot groups according to their Zürich classification in the period 2002–2011.

In the case of the analysed solar plages, they were grouped originally according to a particular classification proposed in 1910 by the director of the Ebro Observatory, Fr. R. Cirera. However, ten years later, the new director of the centre, Fr. L. Rodés, modified the scheme with the addition of an extra type (*diffuse* class). Thus, the inclusion of this new class in 1920 causes a slight decrease of 5–10% in the mean distribution of the rest of types. Notwithstanding this, the most frequent morphology observed in all the considered period is the *cd* Type, which constitutes the transition state between the compact (*c*) and the scattered (*d*) solar plages. Furthermore, these structures present a subtle, more scattered and diffuse trend in the declining phase of practically each solar cycle while at the beginning of the cycles Types *c* and *cd* seem to dominate.

A comparison of the solar activity between sunspots and solar plages in terms of their observed occurrences can be done. Considering the whole studied period, the number of occurrences of solar plages is, on average, about 23% higher than the number of sunspots. This percentage increases to 28% in the 15th solar cycle and declines by up to 19% in the 16th.

With regard to the area analysis, both sunspots and solar plages were grouped, respectively, into four different bins of areas, in order to compare the behaviour of the structures according to their size.

In particular, results confirm that the daily rate of occurrences and the distribution of sunspot groups increase significantly as the area of sunspot groups decreases. Hence, sunspot groups with areas smaller than 70 MSH (Types *I/J,A*) are more common than the rest and are more likely to form, especially near the solar cycle minima.

The same trend has been observed in the occurrences and distributions of solar plage groups up to the solar cycle minimum of 1923. Thus, those groups with areas between 0–70 100 KSH (the smallest groups within Types *cd* and *d*) are the most frequent, notably in and around the solar cycle minima. However, this behaviour begins to change at the beginning of the 16th solar cycle and finally, at the beginning of the 17th solar cycle, it is completely reversed, with those groups within the two largest area bins being more numerous, i.e., solar plages with areas between 150–350 100 KSH and even ones much larger than that. This last result is in line with results obtained by Dara, Macris, and Zachariadis (1975), who observed an increase of 7% in their measurements of solar plage areas from the solar cycle minimum to maximum. They also remarked that smaller groups were predominant during solar cycle minima while in solar cycle maxima, larger groups were more numerous. This fact can also be corroborated by contrasting our results with those obtained by Chatzistergos et al. (2019a, 2019b), after creating a synthetic-composite series from the historical observations of solar plage groups of Arcetri, Kodaikanal, McMath-Hulbert, Meudon, Mitaka, Mt. Wilson, Rome, Schauinsland/Wendelstein and San Fernando observatories. In particular, the annual median value of solar plage areas in disc fractions computed by Chatzistergos et al. (2019a) is of 0.036-disc fractions for the 15th and 16th solar cycle maxima (located in 1917 and 1928, respectively), while in the last solar cycle maximum (1937), the value increases to 0.046-disc fractions. Besides that, our results reveal that in the 15th maximum, the median value of solar plage areas is of 815.57 100 KSH, and the predominant groups are the smallest ones, while the largest are much less common. Nevertheless, in 1928, there was a change

in the general trend, although the median value of areas only increased up to 861.55 100 KSH, larger solar plagues began to be more numerous. Finally, the situation was completely reversed in 1937, and the largest groups became predominant, with the median value of areas being 2097.21 100 KSH.

Finally, an analysis of the N-S asymmetry of all the above properties was carried out. We examined not only the normalized asymmetry index (Letfus, 1960) of all the above properties, but also the significance of the results in terms of excess and probability. This method is based on the Wilson (1987) statistical study of the E-W asymmetry of 850 H $\alpha$  solar flares occurring in 1975, and was also applied by Vizoso and Ballester (1990) to the N-S asymmetry of sunspot areas from the RGO during the period 1874–1976.

The temporal evolution of the normalized asymmetry indices  $\delta$  related to the total number of occurrences of sunspots and solar plagues recorded at the Ebro Observatory during the period 1910–1937 reproduces quite well the general trend observed by analysing the RGO data related to sunspot occurrences (<https://solarscience.msfc.nasa.gov/greenwch.shtml>), and presents a correlation coefficient value of 0.987 in the case of sunspots and of 0.962 for solar plagues. All our results indicate that the northern hemisphere dominates for longer periods of time and shows higher levels of asymmetry. On the contrary, the predominance period of the southern hemisphere is shorter and weaker. In addition, both structures present three noteworthy extremes located in the surroundings of the three solar cycle minima of the studied period, that is: 1912 [S]; 1924 [N]; 1933 [N]. The statistical analysis of these extremes has determined that results are highly significant. Comparable results, including these extremes, were found by Mandal et al. (2017), Mandal, Chatterjee, and Bajernee (2017) in the analysis of the normalized N-S asymmetry index from the yearly averaged sunspot and solar plague area recorded at the Kodaikanal Observatory in the periods 1921–2011 and 1907–1965, respectively.

Focusing on the morphology, the corresponding normalized N-S asymmetry indices associated to sunspots and solar plagues present a similar behaviour regardless of the classification type, and they are akin to the respective global trends, conserving the three remarkable extremes.

Similar conclusions can be extracted by analysing the normalized indices of both structures in terms of the different bins of areas in which they belong. However, it has been observed that larger structures present slightly higher values of the normalized index. This result is corroborated by carrying out the same analysis with the RGO sunspot area data.

Notwithstanding the above, sunspots and solar plague groups do not follow exactly the same general trend with respect to the N-S asymmetry. In comparison with sunspot groups, solar plagues tend to show lower values of the normalized  $\delta$  index in practically all the studied period. This deviation has been observed not only in the Ebro Observatory data, but also in the Royal Greenwich Observatory data. Moreover, similar conclusions can be extracted from the work of Mandal et al. (2017), Mandal, Chatterjee, and Bajernee (2017) by comparing both sunspots and solar plague series from the Kodaikanal Observatory in the period 1921–1965. The normalized asymmetry indices derived from the yearly averaged sunspot and solar plague area also present, on average, lower levels of asymmetry for solar plagues.

Since faculae, and by extension, solar plague groups, are manifestations of dispersing magnetic fields of sunspot groups, the lower N-S asymmetry indices observed in solar plagues in comparison to sunspots could be due to the magnetic field dispersion-driven magnetic cancellation processes, which are more efficient in regions with more closely packed field lines, i.e., on the more active hemisphere. In addition, another factor associated with closely packed magnetic fields is the merging of close-by faculae, thus decreasing their number on the solar surface. Hence, it may very well be that either magnetic cancellation processes or

merger of neighbouring faculae decrease the N-S asymmetry in long-lived faculae and then in solar plages, while in short-lived sunspots such processes have no effect on the asymmetry (Mandal, Chatterjee, and Bajernee, 2017). Notwithstanding the foregoing, different behaviour between sunspots and solar plages were also found in de Paula, Curto, and Casas (2016), concerning the rotation-velocity dependence within the different layers of the solar atmosphere. Mandal, Chatterjee, and Bajernee (2017) showed in their study that sunspots and solar plages are highly correlated with each other on a time scale comparable to the solar cycle, so the two layers are magnetically coupled. In our work, all the Pearson's correlation coefficients are also high since they present values over 0.90. However, the values between sunspots and solar plages are slightly lower in comparison with those computed between two different datasets of sunspots.

Sunspots and solar plages constitute two suitable proxies for studying not only the photosphere and the chromosphere separately, but also the magnetic connection between both layers. Thus, given the importance of understanding these structures, the Ebro Observatory will continue this line of research in the future by analysing other properties and characteristics that can be extracted from our historical daily observations of sunspots and solar plages, such as the morphological evolution of both structures throughout their lifetime.

## 5. Conclusions

In this work, we examined the recently digitalized heliophysics catalogues from the Ebro Observatory in the period 1910–1937. We analysed simultaneously two different solar structures located at different layers of the solar atmosphere: sunspots and solar plages. Our study is focused on the morphological types and areas of these solar structures, analysing and comparing the evolution over time, year by year, of their daily rate of occurrence and their distribution. We also studied the N-S asymmetry. From our findings, we highlight the following results:

- i) In the period 1910–1937, sunspot group occurrences tend to be mostly in the form of Types *I* and *IV* in the Cortie classification, and Types *J*, *A* and *D* in the Zürich classification, especially during the solar maximum of each cycle. These morphological types of sunspot groups consist mainly of small spots with or without penumbra (Types *I/J*, *A*) and bipolar groups whose main spots have penumbra (Types *IV/D*). In respect to solar plage groups, the most frequent morphology is Type *cd*, which is associated to the transition state between compact (*c*) and scattered (*d*) Types. Moreover, solar plages subtly tend to be more scattered and diffuse in the declining phase of practically every solar cycle whereas the *c* and *cd* Types dominate at the beginning of the cycles. Moreover, the solar activity in terms of the total number of occurrences of both phenomena is on average about 23% higher in solar plages than in sunspots during the studied period.
- ii) In general, the occurrence daily rate and the distribution of both structures depend on the area, with the smallest groups the most frequent. In particular, sunspot groups with areas smaller than 70 MSH (Types *I/J*, *A*) and solar plage groups with areas between 0–70 100 KSH (smallest groups within Types *cd* and *d*) respectively, are more likely to appear, especially near the solar cycle minima. We observed in both structures that as the area of the group increases, the occurrence daily rate and distribution decrease. However, this behaviour seems to be reversed completely at the beginning of the 16th and 17th solar cycles in solar plage groups. Moreover, from the 16th solar cycle maxima onwards, larger solar plages begin to be more numerous whereas smaller groups dominate during solar cycle minima.

- iii) With regard to the N-S asymmetry, we observed that the predominance of the northern hemisphere is longer and stronger in comparison with the southern hemisphere, which is characterized with shorter periods of predominance and weaker levels of asymmetry.
- iv) For the period 1910–1937 at least, the normalized N-S asymmetry index  $\delta$  for sunspots and solar plage occurrences follows approximately the same behaviour regardless of the classification type but presents a slight dependence on their area, since both structures show higher values of the N-S asymmetry index, the larger their areas are. Our results are consistent in comparison with the RGO data.
- v) In both structures, and regardless of their morphological type or area, we observed three extremes in the evolution over time of the normalized N-S asymmetry index. These extremes are located in and around the three solar cycle minima of the studied period, that is: 1912 [S]; 1924 [N]; 1933 [N]. The statistical analysis of these extremes has determined that in most of the cases, the results are highly significant. Hence, we can discard randomness in our results. Moreover, in contrast to sunspots, solar plage groups present lower values of the normalized  $\delta$  index in practically all the studied period.
- vi) Finally, the differences observed between both structures, together with the fact that all the Pearson's correlation coefficients between sunspots and solar plagues are slightly lower in comparison with those computed between two different sunspot are relevant enough to deserve further studies.

**Acknowledgements** This work has been possible thanks to the efforts of Ebro Observatory observers and the people who have digitalized our heliophysics bulletins from the beginning of the 20th century. We also want to acknowledge the agencies that run the magnificent portals of WDC-SILSO and NASA's Marshall Space Flight Center Solar Physics Group, providing good quality open access data. Furthermore, authors thank the fruitful comments by the referee.

**Disclosure of Potential Conflicts of Interest** The authors declare that they have no conflicts of interest.

**Publisher's Note** Springer Nature remains neutral with regard to jurisdictional claims in published maps and institutional affiliations.

## References

- Ananthakrishnan, R.: 1952, A note on the observations of sunspots recorded at Kodaikanal from 1903 to 1950. *Kodaikanal Obs. Bull.* **133**, 1.
- Bell, B.: 1962, A long-term North-South asymmetry in the location of solar sources of great geomagnetic storms. *Smithson. Contrib. Astrophys.* **5**, 187.
- Buehler, D., Lagg, A., Solanki, S.K., Van Noort, M.: 2015, Properties of solar plage from a spatially coupled inversion of Hinode SP data. *Astron. Astrophys.* **576**, 27.
- Carbonell, M., Oliver, R., Ballester, J.L.: 1993, On the asymmetry of solar activity. *Astron. Astrophys.* **274**, 497.
- Carrasco, V.M.S., Lefèvre, L., Vaquero, J.M., Gallego, M.C.: 2015, Equivalence relations between the Cortie and Zürich sunspot group morphological classifications. *Solar Phys.* **290**, 1445.
- Chatzistergos, T., Ermolli, I., Krivova, N.A., Solanki, S.K.: 2019a, Analysis of full disc Ca II K spectroheliograms. II. Towards an accurate assessment of long-term variations in plage areas. *Astron. Astrophys.* **625**, 69.
- Chatzistergos, T., Ermolli, I., Falco, M., et al.: 2019b, Historical solar Ca II K observations at the Rome and Catania observatories. *Nuovo Cimento C* **42**, 5.
- Cirera, R.: 1910, Heliófica, Enero 1910. *Bol. Mens. Obs. Ebro* **1**, 21.
- Cortie, A.L.: 1901, On the types of sun-spot disturbances. *Astrophys. J.* **13**, 260.
- Curto, J.J., Solé, J.G., Genescà, M., Blanca, M.J., Vaquero, J.M.: 2016, Historical heliophysical series of the Ebro observatory. *Solar Phys.* **291**, 2587.
- Dara, H.C., Macris, C.J., Zachariadis, T.G.: 1975, Comparison of the dimensions of the flocculi at periods of maximum and minimum solar activity. *Prakt. Akad. Athenon* **50**, 391.

- de Paula, V., Curto, J.J., Casas, R.: 2016, The solar rotation in the 1930s from the sunspot and flocculi catalogs of the Ebro observatory. *Solar Phys.* **291**, 2269.
- Ermolli, I., Marchei, E., Centrone, M., et al.: 2009, The digitized archive of the Arcetri spectroheliograms. Preliminary results from the analysis of Ca II K images. *Astron. Astrophys.* **499**, 627.
- Ermolli, I., Chatzistergos, T., Krivova, N.A., Solanki, S.K.: 2018, The potential of Ca II K observations for solar activity and variability studies. *Proc. Int. Astron. Union* **340**, 115. Long-term Datasets for the Understanding of Solar and Stellar Magnetic Cycles, IAU Symposium.
- García, H.A.: 1990, Evidence for solar-cycle evolution of North-South flare asymmetry during cycles 20 and 21. *Solar Phys.* **127**, 185.
- Gigolashvili, M.Sh., Japaridze, D.R., Mdzinarishvili, T.G., Chargeishvili, B.B.: 2005, N-S asymmetry in the solar differential rotation during 1957–1993. *Solar Phys.* **227**, 27.
- Gonçalves, E., Mendes-Lopes, N., Dorotovič, I., Fernandes, J.M., Garcia, A.: 2014, North and South hemispheric solar activity for cycles 21–23: asymmetry and conditional volatility of plage region areas. *Solar Phys.* **289**, 2283.
- Hathaway, D.H.: 2015, The solar cycle. *Living Rev. Solar Phys.* **12**, 4.
- Howard, R.: 1974, Studies of solar magnetic fields. II – the magnetic fluxes. *Solar Phys.* **38**, 59.
- Joshi, A.: 1995, Asymmetries during the maximum phase of cycle 22. *Solar Phys.* **157**, 315.
- Joshi, B., Pant, P., Manoharan, P.K.: 2006, North-South distribution of solar flares during cycle 23. *J. Astrophys. Astron.* **27**, 151.
- Kleczek, J.: 1953, Relations between flares and sunspots. *Bull. Astron. Inst. Czechoslov.* **4**, 9.
- Kilcik, A., Yurchyshyn, V.B., Abramenko, V., Goode, P.R., Ozguc, A., Rozelot, J.-P., Cao, W.: 2011, Time distributions of large and small sunspot groups over four solar cycles. *Astrophys. J.* **731**, 30.
- Kilcik, A., Ozguc, A., Yurchyshyn, V., Rozelot, J.P.: 2014, Sunspot count periodicities in different Zürich sunspot group classes since 1986. *Solar Phys.* **289**, 4365.
- Kilçik, A., Sahin, S.: 2017, Possible variations in sunspot groups before flaring activity during solar cycles 23 and 24. *Turk. J. Phys.* **41**, 351.
- Kobel, P., Hirzberger, J., Solanki, S.K., Gandorfer, A., Zakharov, V.: 2009, Discriminant analysis of solar bright points and faculae. I. Classification method and center-to-limb distribution. *Astron. Astrophys.* **502**, 303.
- Lefèvre, L., Clette, F.: 2011, A global small sunspot deficit at the base of the index anomalies of solar cycle 23. *Astron. Astrophys.* **536**, L11.
- Lefèvre, L., Clette, F.: 2014, Survey and merging of sunspot catalogs. *Solar Phys.* **289**, 545.
- Lefèvre, L., Aparicio, A.J.P., Gallego, M.C., Vaquero, J.M.: 2016, An early sunspot catalog by Miguel Aguilar for the period 1914–1920. *Solar Phys.* **291**, 2609.
- Lemaire, P.: 2001, Solar chromospheric plage. In: *Encyclopedia of Astronomy and Astrophysics*. Nature Publishing Group and Institute of Physics Publishing.
- Letfus, V.: 1960, Zusammenhang der Asymmetrie der Sonneneruptionen MIT dem 11 jährigen Zyklus. *Bull. Astron. Inst. Czechoslov.* **11**, 31.
- Mandal, S., Hegde, M., Samanta, T., Hazra, G., Banerjee, D., Ravindra, B.: 2017, Kodaikanal digitized white-light data archive (1921–2011): analysis of various solar cycle features. *Astron. Astrophys.* **601**, 106.
- Mandal, S., Chatterjee, S., Bajernee, D.: 2017, Association of plagues with sunspots: a multi-wavelength study using Kodaikanal Ca II K and Greenwich sunspot area data. *Astrophys. J.* **835**, 158.
- McIntosh, P.S.: 1990, The classification of sunspot groups. *Solar Phys.* **125**, 251.
- Mursula, K., Hiltula, T.: 2003, Bashful ballerina: southward shifted heliospheric current sheet. *Geophys. Res. Lett.* **30**, 2.
- Newton, H.W., Milsom, A.S.: 1955, Note on the observed differences in spottedness of the Sun's northern and southern hemispheres. *Mon. Not. Roy. Astron. Soc.* **115**, 398.
- Oh, S., Chang, H.: 2012, Change of sunspot groups observed from 2002 to 2011 at Butterstar observatory. *J. Astron. Space Sci.* **29**, 245.
- Oliver, R., Ballester, J.L.: 1994, The North-South asymmetry of sunspot areas during solar cycle 22. *Solar Phys.* **152**, 481.
- Righini, G., Godoli, G.: 1950, The physical meaning of the character figures of solar phenomena. *J. Geophys. Res.* **55**, 415.
- Rodés, L.: 1920, Heliofísica, Enero 1920. *Bol. Mens. Obs. Ebro* **11**, 3.
- Romañá, A.: 1942, Heliofísica, Enero 1942. *Bol. Mens. Obs. Ebro* **30**, 1.
- Romañá, A.: 1947, Heliofísica, Diciembre 1947. *Bol. Mens. Obs. Ebro* **35**, 195.
- Roy, J.R.: 1977, The North-South distribution of major solar are events, sunspot magnetic classes and sunspot areas (1955–1974). *Solar Phys.* **52**, 53.
- Seguí, A., Curto, J.J., de Paula, V., Vaquero, J.M., Rodríguez-Gasén, R.: 2019, Temporal variation and asymmetry of sunspot and solar plage types from 1930 to 1936. *Adv. Space Res.* **63**, 3738.
- Solanki, S.K.: 2003, Sunspots: an overview. *Astron. Astrophys. Rev.* **11**, 153.

- Song, W.B., Wang, J.X., Ma, X.: 2005, A study of the North-South asymmetry of solar photospheric magnetic flux. *Chin. Astron. Astrophys.* **29**, 274.
- Stephenson, F.R.: 1990, Historical evidence concerning the Sun; interpretation of sunspot records during the telescopic and pretelescopic eras. *Phil. Trans. Roy. Soc. London Ser. A, Math. Phys. Sci.* **330**, 499.
- Swinson, D.B., Koyama, H., Saito, T.: 1986, Long-term variations in North-South asymmetry of solar activity. *Solar Phys.* **106**, 35.
- Temmer, M., Veronig, A., Hanslmeier, A., Otruba, W., Meserotti, M.: 2001, Statistical analysis of solar H $\alpha$  flares. *Astron. Astrophys.* **375**, 1049.
- Temmer, M., Rybák, J., Bendík, P., Veronig, A., Vogler, F., Otruba, W., Pötzi, W., Hanslmeier, A.: 2006, Hemispheric sunspot numbers R<sub>n</sub> and R<sub>s</sub> from 1945–2004: catalogue and N-S asymmetry analysis for solar cycles 18–23. *Astron. Astrophys.* **447**, 735.
- Udías, A.: 2003, *Searching the Heavens and the Earth: The History of Jesuit Observatories, Astrophysics and Space Science Library*. Kluwer Academic, Dordrecht.
- Vaquero, J.M., Gallego, M.C., Acero, F.J., García, J.A.: 2007, *Spectroheliographic Observations in Madrid (1912–1917). The Physics of Chromospheric Plasmas, ASP Conference Series* **368**, 17.
- Verma, V.K.: 1992, The distribution of the North-South asymmetry for the various activity cycles. In: *The Solar Cycle, ASP Conference Series* **27**, 429.
- Verma, V.K.: 2000, On the distribution and asymmetry of solar active prominences. *Solar Phys.* **194**, 87.
- Vizoso, G., Ballester, J.L.: 1987, North-South asymmetry in sudden disappearances of solar prominences. *Solar Phys.* **112**, 317.
- Vizoso, G., Ballester, J.L.: 1990, The North-South asymmetry of sunspots. *Astron. Astrophys.* **229**, 540.
- Waldmeier, M.: 1947, *Publ. Zür. Obs.* **9**, 1.
- Waldmeier, M.: 1955, *Ergebnisse und Probleme der Sonnenforschung*, Geest & Portig, Leipzig.
- Waldmeier, M.: 1971, The asymmetry of solar activity in the years 1959–1969. *Solar Phys.* **20**, 332.
- Wang, Y.M., Robbrecht, E.: 2011, Asymmetric sunspot activity and the southward displacement of the heliospheric current sheet. *Astrophys. J.* **736**, 136.
- Weiss, N.: 2001, Sunspots. In: *Encyclopedia of Astronomy and Astrophysics*. Nature Publishing Group and Institute of Physics Publishing.
- Wilson, R.M.: 1987, Statistical Aspects of Solar Flares. NASA Technical Paper 2714.
- Zhang, L.: 2012, *Solar Active Longitudes and Their Rotation, Report Series in Physical Sciences* **78**, University of Oulu, Oulu.